

**CHARACTERIZATION OF THE INTERACTION BETWEEN TRPA1 AND
CREATINE KINASE**

**A THESIS SUBMITTED TO THE GRADUATE DIVISION OF THE UNIVERSITY
OF HAWAII IN PARTIAL FULFILLMENT OF THE REQUIREMENTS FOR THE
DEGREE OF**

MASTER OF SCIENCE

IN

CELL AND MOLECULAR BIOLOGY

DECEMBER 2007

By

Kimberly Eileen Maile Cochrane

Thesis Committee:

Alan F. Lau, Chairperson

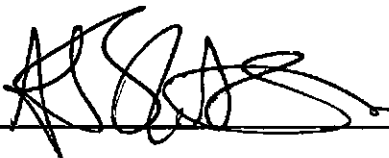
Heinz Gert de Couet

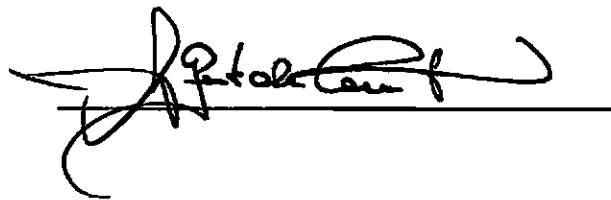
Alexander James Stokes

We certify that we have read this thesis and that, in our opinion, it is satisfactory in scope and quality as a thesis for the degree of Master of Science in Cell and Molecular Biology.

THESIS COMMITTEE


Chairperson





ACKNOWLEDGEMENTS

Thank you to:

- **My advisors, Dr. Alexander Stokes and Dr. Helen Turner for sharing their knowledge, enthusiasm and guidance.**
- **The members of the thesis committee, Dr. Alan Lau and Dr. Heinz Gert de Couet for their time and assistance.**
- **Mr. Clay Wakano, Mrs. Lori Shimoda, Dr. Annette Lis and the other members of The Queen's Center for Biomedical Research that helped me out along the way.**
- **Dr. Andrea Fleig and Dr. Reinhold Penner for facilitating the completion this project.**
- **Dr. Mariana Gerschenson for generous support, friendship and for introducing me to the CMB program.**
- **My Parents and John Stepien for their financial and emotional support.**

This project was supported by funding from:

The Queen Emma Research Fund (PA# 2005-127)

The National Institute of Health (grant #5RO1GM070634)

The Queen's Medical Center

The Cell and Molecular Biology Program at the University of Hawai'i at Manoa

ABSTRACT

The ankyrin-like transient receptor channel (TRPA1) is a member of the TRP channel family of proteins that regulate vital cell functions by increasing cell membranes permeability to cations in response to a diverse array of stimuli. TRPA1 proteins form transmembrane channels that regulate intracellular calcium levels in neuronal cells in response to a variety of sensory signals. Results presented in this thesis confirm the presence of TRPA1 protein in non-neuronal human cells. Evidence of TRPA1 protein in subcellular human cell fractions containing intracellular membranes is also presented. In addition, a novel interaction between over-expressed human TRPA1 and creatine kinase proteins is identified in human cell lysate. These findings suggest that in addition to its role as a neurosensor, TRPA1 may play a role in the regulation of essential cell processes.

TABLE OF CONTENTS

ACKNOWLEDGEMENTS	iii
ABSTRACT	iv
TABLE OF CONTENTS	v
LIST OF TABLES	vii
LIST OF FIGURES.....	viii
LIST OF COMMONLY USED ABBREVIATIONS	x
CHAPTER 1: GENERAL INTRODUCTION	1
1.1 The Transient Receptor Potential (TRP) Channel Family	1
1.2 TRPA1	4
1.3 Preliminary Data.....	9
1.4 Hypothesis and Goals	13
CHAPTER 2: MATERIALS AND METHODS.....	15
2.1 Tools Available in the Laboratory	15
2.2 Molecular Biology	16
2.3 Protein Expression and Biochemistry.....	26
2.4 Cell Biology	31
CHAPTER 3: TRPA1 INTERACTS WITH HUMAN CREATINE KINASES	35

3.1 Introduction	35
3.2 Results	36
3.3 Discussion	48
<u>CHAPTER 4: LOCALIZATION OF TRPA1 EXPRESSION</u>	51
4.1 Introduction	51
4.2 Results	52
4.3 Discussion	58
CHAPTER 5: DEVELOPMENT OF TOOLS FOR FURTHER STUDY OF THE INTERACTION BETWEEN TRPA1 AND CREATINE KINASE	62
5.1 Introduction	62
5.2 Results	63
5.3 Discussion	74
CHAPTER 6: SUMMARY DISCUSSION	76
APPENDIX A	82
APPENDIX B	85
REFERENCES	88

LIST OF TABLES

Table 2.1. Sources of cDNA..... 16

Table 2.2. PCR primers.20

Table 2.3. Sequencing primers.....25

Table 2.4. Antibodies.30

LIST OF FIGURES

Figure 1.1. Structure of monomeric TRP protein and functional tetrameric channel.....	3
Figure 1.2. Phylogenetic tree of TRPA1 homologues.....	5
Figure 1.3. CKB abolishes isoproterenol-induced TRPA1 currents.	12
Figure 2.1. pTrcHisB vector map.....	17
Figure 2.2. pcDNA 4/TO vector map.....	18
Figure 3.1. Western blot showing co-immunoprecipitation of V5-CKB by FLAG- TRPA1.	37
Figure 3.2. V5-tagged creatine kinase PCR products.	39
Figure 3.3. CK-V5 sub-cloning strategy.	40
Figure 3.4. Restriction enzyme digested CKM- and CKMT1B-pcDNA4/TO constructs.	41
Figure 3.5. Restriction enzyme digested CKMT2-pcDNA4/TO constructs.....	42
Figure 3.6. V5-CK insert and restriction enzyme digested CK-pcDNA4/TO constructs.	43
Figure 3.7. Western blot showing co-immunoprecipitation of V5-CKM by FLAG- TRPA1.	45
Figure 3.8. Western blot showing V5-CKMT1B co-immunoprecipitation by FLAG- TRPA1.	46
Figure 3.9. Western blot showing V5-CKMT2 co-immunoprecipitation by FLAG- TRPA1.	47
Figure 4.1. Enriched TRPA1 protein expression in subcellular PM/ER fractions.	53

Figure 4.2. High MW TRPA1 protein expression is enriched in mitochondrial fractions.	55
Figure 4.3. TRPA1 protein expression in human tissue lysates.	57
Figure 5.1. Kyte/Doolittle hydropathy plot prediction of TRPA1 transmembrane domains.	64
Figure 5.2. pTrcHisB vector subcloning schematic.	65
Figure 5.3. Enzymatic digest of CKM, TRPA1-N and TRPA1-C pTrcHisB constructs.	66
Figure 5.4. CKM protein expression and purification Coomassie blue stained gel.....	69
Figure 5.5. CKM protein expression and isolation western blot.	71
Figure 5.6. TRPA1 C-terminal protein expression and isolation western blot.....	72
Figure 5.7. TRPA1 N-terminal protein expression and isolation western blot.....	73
Figure 6.1. Summary graphic.....	77
Figure A.1 Changes in FURA-2 AM absorbance in BITC-stimulated AFC cells.....	84
Figure B.1. Preliminary <i>in vitro</i> affinity binding assay.....	87

LIST OF COMMONLY USED ABBREVIATIONS

AFC	TRPA1-FLAG over-expressing HEK293TREx
bp	base pair
BSA	bovine serum albumin
Ca ²⁺	divalent calcium ions
cDNA	coding deoxyribonucleic acid
CK	creatine kinase
CKB	brain type creatine kinase
CKM	muscle type creatine kinase
CKMT1B	ubiquitous mitochondrial creatine kinase
CKMT2	sarcomeric mitochondrial creatine kinase
C-term	carboxyl terminus
DNA	deoxyribonucleic acid
<i>E. coli</i>	<i>Escherichia coli</i>
ECL	enhanced chemiluminescence
EDTA	ethylenediamine tetra-acetic acid
EGTA	[ethylene-bis(oxyethylenitrilo)] tetra-acetic acid
ER	endoplasmic reticulum
x g	relative centrifugal force (RCF)
HEK	human embryonic kidney cells
HEK293TREx	HEK cells stably expressing the 4/TO TREx vector

HEPES	N-2-hydroxyethylpiperaxine-N'-2-ethanesulphonic acid
His	histidine
hr	hour(s)
HRP	horseradish peroxidase
IPTG	isopropyl-2-D-thiogalactopyranosidde
kb	kilo bases
kDa	kilo daltons
LB	Luria-Bertani
M	molar
min	minute(s)
MOPS	4-morpholineproopanesulphonic acid
MW	molecular weight
N-term	amino terminus
OD	optical density
PAGE	polyacrylamide gel electrophoresis
PBS	phosphate buffered saline
PCR	polymerase chain reaction
PDH	pyruvate dehydrogenase
PM	plasma membrane
RSB	reducing sample buffer
RT	room temperature
SDS	sodium dodecyl sulphate

sec	second(s)
SRS	Sos recruitment system
TAE	tris/acetate/EDTA buffer
Tris	tris(hydroxymethyl)aminomethane
TRP	transient receptor potential
TRPA1	human TRP cation channel, subfamily A, member 1
Y2H	yeast two-hybrid

CHAPTER 1: GENERAL INTRODUCTION

1.1 The Transient Receptor Potential (TRP) Channel Family

Transient receptor potential (TRP) channels function as physiological sensors for a diverse array of stimuli including, touch, temperature, taste, pain, osmolarity, and pheromones. They form transmembrane channels associated with acute signaling events that involve the rapid transport of cations across cell membranes. Monovalent and divalent cations can traverse cell membranes through TRP channels, which work directly as channels in cell membranes, and indirectly through changes in membrane polarization that modulate the driving force for cation entry by alternative pathways. Molecular cloning and electrophysiological study have produced extensive amounts of data on the roles of TRP channels in a variety of tissues. Despite this, the regulation and physiological functions of TRP channels are in many cases still unclear.

The TRP designation is attributed to a spontaneously occurring *Drosophila* gene mutation. Mutations in a *Drosophila trp* gene result in disruption of a Ca^{2+} entry channel in photoreceptor cells. This leads to a transient light-induced current, in response to a sustained light stimulus. The responsible gene was termed *trp*, for transient receptor potential. The initial discovery of TRP channels has been followed by findings that TRP channels are expressed in many organisms, tissues and cell types. Evidence continues to grow in support of a high level of evolutionary conservation amongst TRP channels and their physiological roles. (Clapham, 2003; Clapham et al., 2001; Minke and Cook, 2002; Peretz et al., 1994)

There are seven distinct TRP channel subfamilies based on amino acid homology. Only six of these subfamilies have been identified in mammals. (Nilius, 2007) All members of the TRP channel family contain a transmembrane region typical of channel proteins that consists of six alpha-helical transmembrane segments S1-S6 and the pore region (P) loop, between segments S5 and S6. In addition, all TRP channels have intracellular amino (NH₂) and carboxyl (COOH) termini. Functional cation-selective TRP channels result from the assembly of activated TRP channel subunits into homo- or hetero-tetramers in both excitable and non-excitable cells (Figure 1.1). (Clapham, 2003; Minke and Cook, 2002; Montell, 2001; Pedersen et al., 2005; Ramsey et al., 2006; Venkatachalam and Montell, 2007)

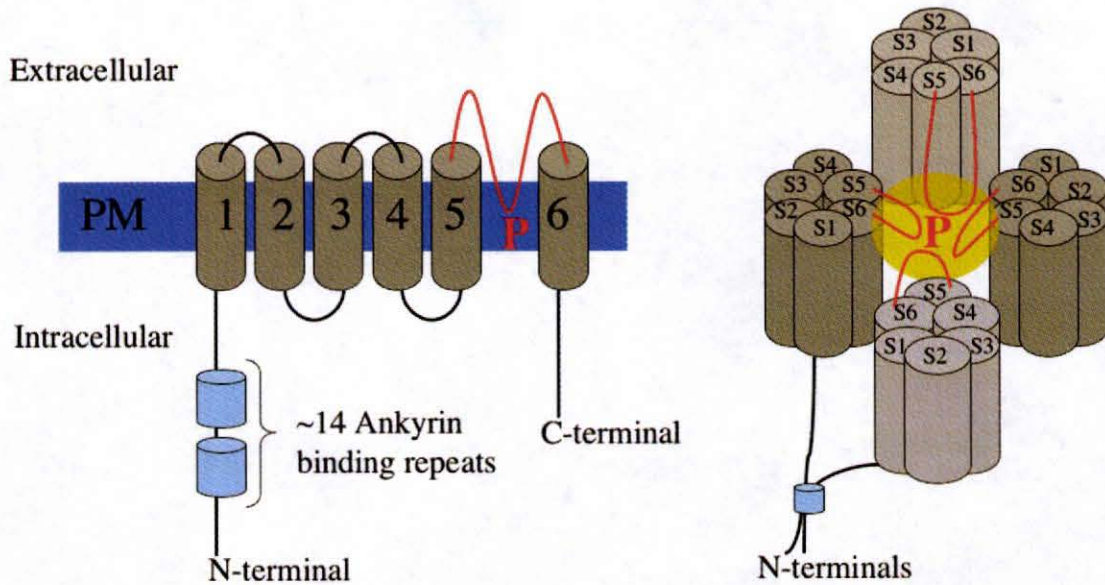


Figure 1.1. Structure of monomeric TRP protein and functional tetrameric channel.

Monomeric TRP channel proteins shown on the left contain six alpha-helical segments that traverse the plasma membrane (PM) with a pore region loop (P) between segments 5 and 6. Amino (N) and carboxyl (C) terminals are cytoplasmic. Some TRP proteins, including TRPA1 contain N-terminal ankyrin repeat domains. Functional channels shown on the right consist of homo- or hetero-tetramers. Pore region loops form the central cation selective pore (shaded region) and amino terminals might also interact.

The diversity of TRP channel morphology allows them to mediate the flow of ions across cell membranes in response to a variety of stimuli, including, the binding of intracellular and extracellular chemical messengers, changes in temperature, changes in osmotic or mechanical stress and the depletion of intracellular Ca^{2+} stores. Due to their diversity, defects in the function of TRP channels can affect a vast number of cellular and systemic processes that rely on cations as signaling molecules. Increased understanding

the specific functions of TRP channels will aid in the identification and treatment of the effects of TRP channel dysfunctions. (Clapham, 2003; Nilius, 2007)

1.2 TRPA1

Ankyrin-like TRP, known as TRPA1 (also ANKTM1), is the only member of the TRPA subfamily in mammals. The TRPA subfamily is named for the chain of (~14) ankyrin repeat domains in the amino terminus, shown in Figure 1.1. Ankyrin repeat domains, which are also found in other TRP channels, are known to function as protein-protein interaction domains. The human gene for TRPA1 is located on chromosome 8 in band 8q13 and encodes a protein of 1119 amino acids with a predicted atomic mass of 127 kDa (MacVector software prediction confirmed by Western Blot). TRPA1 is Ca²⁺ selective and contains an amino terminal EF hand calcium control element that is critical for channel function. (Doerner et al., 2007; Zurborg et al., 2007)

Homologues of the mammalian TRPA1 protein are found in nematode, drosophila, and many other distantly related organisms demonstrating a deep-rooted ancestral lineage. (Saito and Shingai, 2006) The widespread conservation of TRPA1 protein suggests that it plays an important functional role (Figure 1.2).

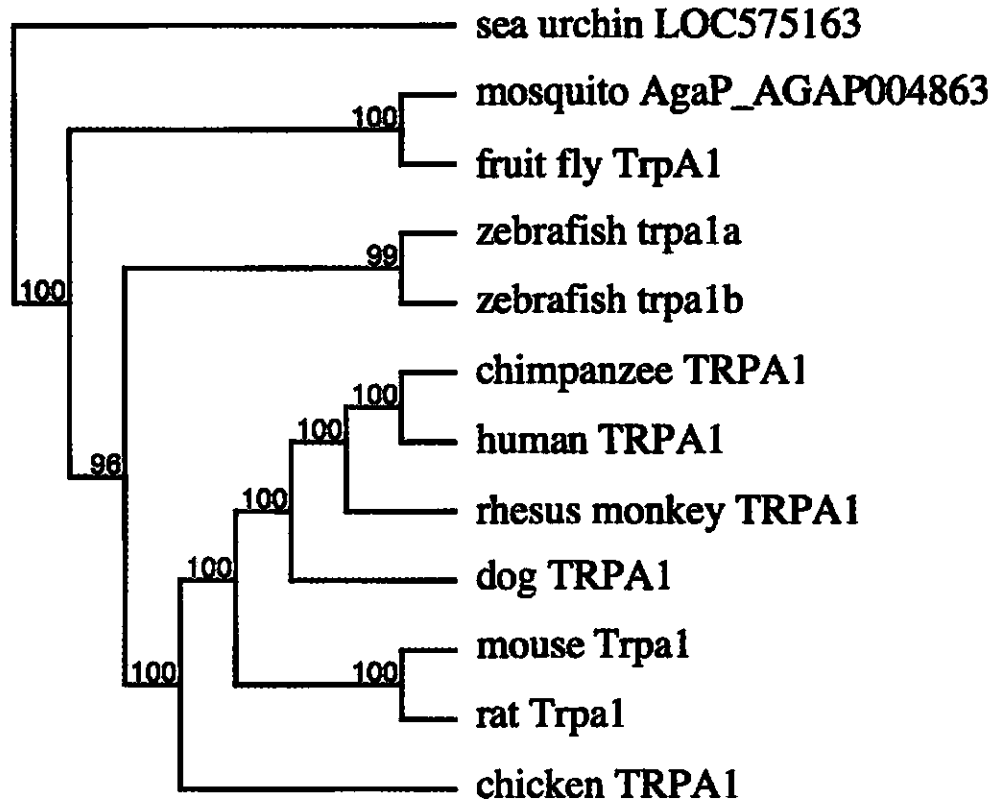


Figure 1.2. Phylogenetic tree of TRPA1 homologues.

This phylogenetic tree was reconstructed based on alignment of TRPA1 nucleotide sequences from included organisms. Nucleotide sequences were obtained from the NCBI GenBank database. MacVector software (Accelrys, 2001) was used to generate a ClustalW multiple sequence alignment and phylogenetic tree. The tree was built using the neighbor joining best tree method with systemic tie-breaking and proportional gap distribution. The pairwise distances between sequences were determined using the Tamura-Nei method. Branches are rooted by outgroups. Bootstrap values on branches estimate the confidence value assigned to the corresponding nodes. Evolutionary conservation of TRPA1 protein is demonstrated by the variety of distantly related species in which TRPA1 is expressed.

The TRPA1 channel was first identified in lung fibroblasts, where it was proposed that altered regulation of the channel was linked to oncogenic transformation status. (Jaquemar et al., 1999) Since then, TRPA1 has been identified in many cell types. Little is known about the regulation and physiological functions of TRPA1 outside of neurons because the study of TRPA1 has been focused almost entirely on its sensory roles in nociceptive neurons. Several neurosensory roles have been proposed for TRPA1, some of which remain controversial.

It has been concluded that TRPA1 plays a role in neurogenic inflammation and pain hypersensitivity when activated by a variety of noxious chemicals, environmental irritants and pro-algesic or pro-inflammatory agents. Isothiocyanates are pungent natural compounds derived from compounds such as garlic, wasabi oil, mustard oil, cinnamon and horseradish that activate TRPA1 and elicit pain and inflammation. This role is confirmed by the finding that *Trpa1* knockout mice display reduced behavioral aversion responses to the application of mustard oil on their hind paw. The activation of TRPA1 channels (in rat trigeminal neurons, *Xenopus* oocytes and human embryonic kidney cells) by isothiocyanates is not detected upon removal of extracellular calcium, demonstrating functional localization of TRPA1 in the plasma membrane. (Jordt et al., 2004) Recent research has shown that structurally diverse thiol-reactive compounds activate TRPA1 in a manner that relies on covalent modification of cysteine residues within the cytoplasmic N terminus of the channel. (Hinman et al., 2006; Kim and Cavanaugh, 2007; Macpherson et al., 2007)

Studies in knockout mice and adult rat dorsal root ganglion neurons shown that TRPA1 is also activated through G protein-coupled receptor phospholipase C-coupled signaling pathways in response to activation by proalgesic and proinflammatory agents like bradykinin. (Bandell et al., 2004; Bautista et al., 2006) This activation mechanism is shared by other TRP channels that rely on activation by one or more of the lipid products of phospholipase C.

TRPA1 also functions as a sensor of noxious cold. Temperatures less than 17°C, have been shown to elicit a rise in intracellular calcium concentrations in TRPA1-expressing rat dorsal root ganglion cells. The role of TRPA1 as a sensor of cold temperatures is further supported by the fact that the channel protein is highly expressed with other nociceptive markers including TRPV1 and TRPM8, and is activated by the synthetic cold mimetic compound icilin. (Moran et al., 2004; Story et al., 2003) In addition, *Trpa1*-deficient mice demonstrate a reduced behavioral response to the cooling sensation resulting from the administration of acetone to the hind paw. (Kwan et al., 2006) However, cultured trigeminal neurons from *Trpa1*-deficient mice show no significant difference in the prevalence of cold sensitive neurons or their response to temperatures as low as 6°C. (Bautista et al., 2006) More recently, it has been proposed that TRPA1 currents associated with cold sensation may result indirectly through activation of the EF-hand (calcium binding) domain of TRPA1 by increased intracellular calcium concentrations. (Bautista et al., 2006; Zurborg et al., 2007) There is still debate in regard to the mechanism by which TRPA1 functions in thermosensation.

The identification of TRPA1 homologues in hearing cells of bullfrog and mouse suggested that, TRPA1 could also play a mechanosensory role in hearing. Disruption of TRPA1 expression in zebrafish and mice by morpholino oligonucleotides resulted in a reduction of transduction channel function in mice. Researchers proposed that the long chain of amino-terminal ankyrin repeats actually form the elastic element that stretches when hair cell's cilia move, resulting in detection and amplification of sounds. Recent research demonstrates unimpaired balance and auditory function (noise-evoked startle response) in *Trpa1*-deficient mice and in mice in which the essential exons for *Trpa1* gene function were deleted. (Bautista et al., 2006; Corey et al., 2004) This discovery, along with the observance of functional cochlea and utricle cells have led to the conclusion that TRPA1 is not an essential component of the mouse hair cell transduction channel.

Amphipathic molecules have been shown to modulate the activity of TRPA1 (and other mechanosensitive ion channels) by causing curvature on the cell membrane due to charge-dependent partitioning in the inner or outer sheets of the lipid bilayer. (Hill and Schaefer, 2007) TRPA1 knockout mice also display a reduced behavioral response to noxious, punctate, cutaneous, mechanical stimuli, suggesting a role in mechanosensory role in the peripheral sensory system. Controversy still exists as to the possible role of TRPA1 in mechanosensation.

Numerous papers have been published related to the aforementioned sensory roles of TRPA1 in the plasma membrane of neurons. In contrast, the roles of TRPA1 in non-neuronal cells and in other intracellular membranes have just begun to be explored. The

expression of TRPA1 in multiple tissues and cell types, suggests that it may have other functions in addition to neurosensation. Recently it was proposed that TRPA1 exerts an important role in urinary bladder function because its activation causes a graded contraction of the rat urinary bladder *in vitro* that is dependent on the influx of extracellular calcium. (Andrade et al., 2006)

Levels of TRPA1 protein are altered in many human cancers, which may be related to the interaction between TRPA1 protein and the tumor-suppressor protein cylindromatosis (CYLD). Over-expression of the CYLD enzyme suppresses the ubiquitination of TRPA1 shown to occur after icilin-induced stimulation in TRPA1-FLAG-HEK293TREx cells. In addition, the over-expression of CYLD in HEK293 cells extends the lifetime of TRPA1 protein. Termination of the association between CYLD and TRPA1 is proposed to be a component of the signal termination mechanism for TRPA1. (Stokes et al., 2006)

Preliminary evidence generated in our lab has identified a novel TRPA1 protein interaction that may be involved in its regulation. Evidence of this interaction, as well as the identification of TRPA1 protein in novel cellular locations suggest yet another functional role for TRPA1.

1.3 Preliminary Data

The activity of ion channels is often regulated via direct interaction with other intracellular proteins. The Sos recruitment yeast two-hybrid system (SRS) was used to identify a series of potential binding partners for TRPA1. The SRS is a type of yeast-two

hybrid assay that is used to identify potential interactions between proteins expressed in yeast. Functional activation of the Ras signaling pathway, by the yeast Ras guanyl nucleotide exchange factor (GEF), is essential for the viability of the yeast *Saccharomyces cerevisiae*. The SRS takes advantage of a specific strain of the yeast *Saccharomyces cerevisiae* that shows temperature sensitive growth resulting from a point mutation in the yeast Ras GEF. Growth at the non-permissive temperature is restored by expression of the mammalian GDP-GTP exchange factor hSos that is artificially targeted to the plasma membrane, where it can activate Ras. The SRS system involves the expression of the target protein fused to Sos and fusion of the potential partner proteins to a membrane localization signal. Interactions between the target and partner proteins recruit Sos to the plasma membrane, resulting in Ras activation and cell growth. (Van Crielinge and Beyaert, 1999)

The tumor suppressor CYLD was identified by the SRS as a potential binding partner for TRPA1. This interaction was confirmed through co-immunoprecipitation. Furthermore, it was demonstrated that TRPA1 is a substrate for the de-ubiquitinating activity of this enzyme and that suppression of TRPA1 ubiquitination by CYLD results in increased cellular levels of TRPA1. The ubiquitination of TRPA1 is predicted to influence inactivation, internalization and recycling of the protein after stimulation. (Stokes et al., 2006)

Another potential TRPA1 binding partner identified by the SRS is the brain-specific isotype of creatine kinase (CKB). Characterization of this potential interaction will provide information about TRPA1 that could be of functional importance. Creatine

kinase is an enzyme that controls cellular energy homeostasis by reversible conversion of creatine into phosphocreatine. There are four creatine kinase isozymes; Brain-type (B), muscle-type (M), and two mitochondrial forms; ubiquitous (CKMT1) and sarcomeric (CKMT2), which exist in two homo- or hetero-meric forms; as dimers or octamers. (Schnyder et al., 1994)

Preliminary electrophysiological data from single cell patch clamp experiments performed by Dr. Andrea Fleig, suggests that addition of muscle-type creatine kinase (2 U/ml) to the internal patch solution abolishes the TRPA1 current that is present in control cells (Figure 1.3). Human embryonic kidney cells stably over-expressing TRPA1 in a tetracycline-inducible expression vector (see AFC cells in Materials and Methods) were induced with tetracycline (1 $\mu\text{g}/\mu\text{l}$) for 16 h at 37°C. The whole-cell patch clamp configuration was used to measure TRPA1 currents. External conditions were as follows 1 mM CaCl₂, 140 mM NaCl, 2.8 mM KCl, 2 mM MgCl₂, 10 mM HEPES NaOH, 10 mM glucose, and internal conditions were 140 mM Kglucose, 8 mM NaCl, 1 mM MgCl₂, 10 mM HEPES NaOH, 10 mM K-BAPTA, 2 mM MgATP, 0.5 mM NaGTP plus experimental compounds. The addition of 2 U/ml muscle creatine kinase (native), 3 mM MgATP, 0.5 mM GTP abolishes the signature TRPA1 conductance in response to isoproterenol that is present in control cells. The potential regulation of TRPA1 by creatine kinase implies that TRPA1 may be involved in fundamental cellular processes directly linked to energy homeostasis.

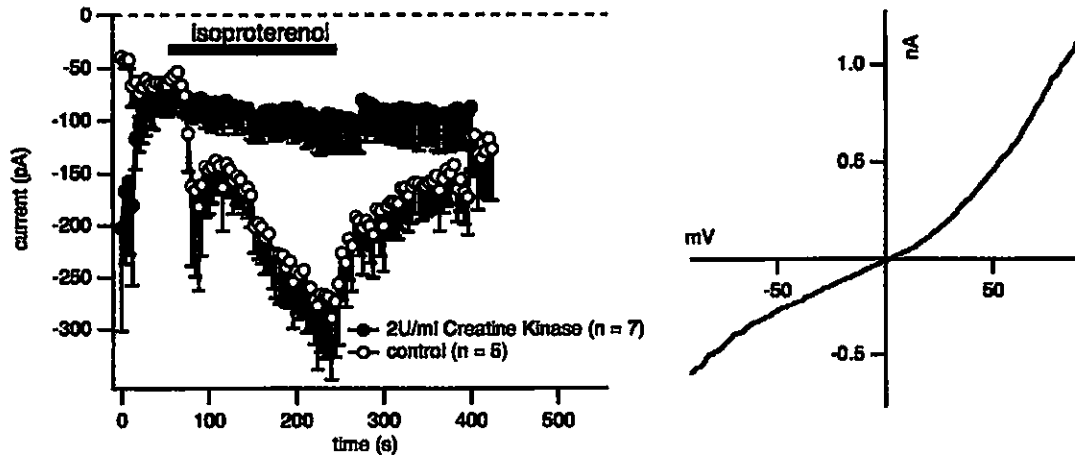


Figure 1.3. CKB abolishes isoproterenol-induced TRPA1 currents.

Left panel: Average TRPA1 current densities at -80mV in HEK293TREx cells stably expressing TRPA1. Black bar indicates the application of isoproterenol (300 μ M) using a wide-tipped perfusion pipette. Error bars indicate SEM. Current in response to application of isoproterenol in control cells (n = 5) indicated by open circles. Filled circles indicate lack of isoproterenol-induced response (n = 7) when 2 U/ml muscle-type creatine kinase is present in the internal patch solution.

Right panel: Example current-voltage relationship of isoproterenol-induced TRPA1 current from a representative control cell shown in the left panel. These experiments were performed by Dr. Andrea Fleig.

Fluctuating calcium levels are a common factor in a vast array of signaling cascades that are central to regulating cellular energy homeostasis. Certain organelles, including the endoplasmic reticulum (ER), Golgi apparatus, nucleus and mitochondria, serve as storage compartments for calcium within the cell. Specialized channels in the membranes of these organelles and at the plasma membrane generate calcium currents of the appropriate duration and magnitude in response to various stimuli. Preliminary electron microscopy data from our lab (not shown) suggests that in addition to expression

in the plasma membrane, TRPA1 is expressed in mitochondrial membranes. Mitochondria can function as localized calcium stores that have been shown to control a range of vital calcium-dependent signaling cascades, including those central to apoptotic cell death. (Jacobson and Duchen, 2004; Nicholls, 2005; Parekh, 2003) Based on the potential location of TRPA1 in the mitochondria, there is a possibility that it could be directly involved in the regulation of cellular energy homeostasis.

1.4 Hypothesis and Goals

This thesis will begin to address the following hypotheses based on the previous results from our laboratory and the current literature regarding TRPA1:

1. TRPA1 protein interacts with human creatine kinase proteins.

The goal is to validate the interaction between human TRPA1 protein and the four human creatine kinase protein isoforms in a human cell environment. Future research could validate the interaction between the endogenous proteins *in vivo* and further characterize the interaction.

2. TRPA1 protein is expressed in mitochondria.

The goal is to determine whether TRPA1 protein is expressed in subcellular human cell fractions that contain mitochondrial proteins. Future research could further characterize the TRPA1 protein expression pattern and channel activity in newly identified subcellular locations.

3. TRPA1 protein interacts directly with muscle-type creatine kinase protein.

The goal is to generate histidine-tagged creatine kinase and TRPA1 terminal peptides.

Future research could employ these proteins to characterize the nature of the interaction between creatine kinase and TRPA1.

CHAPTER 2: MATERIALS AND METHODS

2.1 Tools Available in the Laboratory

TRPA1 antibody. Polyclonal rabbit antibody was raised against the carboxyl-terminal cytoplasmic peptide tail of the endogenous human TRPA1 protein with technical support from Bethyl Laboratories, Inc. in Texas. The antigenic peptide sequence consists of residues 1071-1090 (KMEISETEDDDSHCSFQDR). The antibody purification and titer were determined by ELISA and its ability to detect TRPA1 in both native (immunoprecipitation) and SDS-denatured (western blot) conformations were validated in the AFC cell line (see description below).

HEK293TREx cell line. Invitrogen's T-REx™ System (Invitrogen, CA) is a tetracycline regulated mammalian expression system. The system utilizes a repressor mechanism to block transcription from the CMV promoter in the absence of tetracycline.

AFC cell line. HEK293TREx stable cell line (Invitrogen) that expresses a FLAG-TRPA1 fusion protein upon tetracycline induction. The pcDNA 5/TO vector (Invitrogen) was used in the production of this cell line.

V5-CKB. Human Brain type creatine kinase subcloned in a pcDNA4/TO vector (Invitrogen) with an N-terminal V5 epitope tag.

Table 2.1. Sources of cDNA.

cDNA	Source	NCBI accession #
CKM	Open Biosystems	BC007462
CKB	A. J. Stokes	NM001823
CKmt1B	Open Biosystems	NM020990
CKmt2	Open Biosystems	BC029140
TRPA1/ANKTM1	A. J. Stokes (Dr Beat Trueb, U. of Berne)	NM007332

2.2 Molecular Biology

Imaging. Visualization of DNA separated by Agarose gel electrophoresis was performed on the Molecular Imager Gel Doc XR system with Quantity One 1-D analysis software. The mass of DNA in samples was approximated using a 1 kb DNA ladder (New England BioLabs Inc. (NEB), MA).

Vector maps. During the course of the work presented in this dissertation, cDNAs of interest were subcloned into pTrcHisB and pcDNA4/TO plasmid vectors (Invitrogen, CA). Maps of these vectors from the Invitrogen website are shown in Figures 2.1 and 2.2.

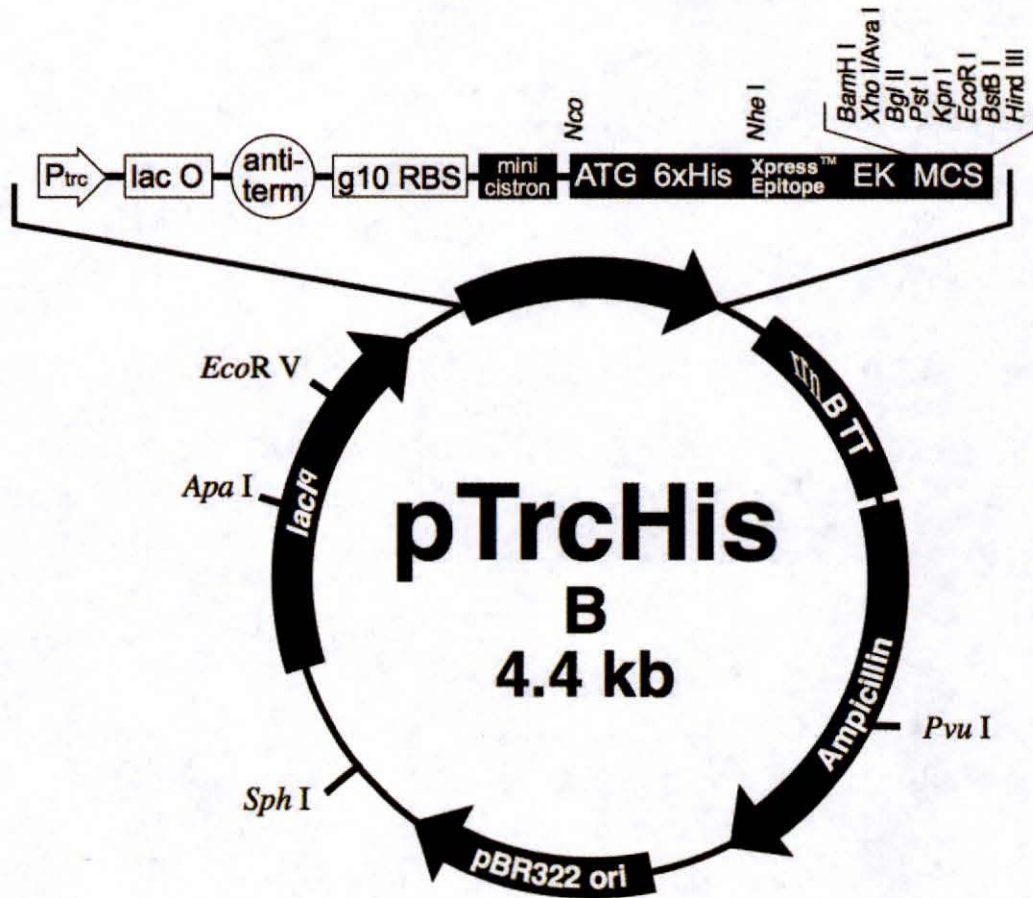


Figure 2.1. pTrcHisB vector map.

pTrcHisB is a pBR322-derived expression vector designed for efficient recombinant protein expression and purification in *E. coli*. The *trc* (*trp-lac*) promoter and the *rrnB* anti-termination region allow high levels of protein expression. The vector also contains the *lacI^f* gene, which codes for the *lac* repressor protein that allows for efficient repression of transcription of the cloned insert in *E. coli*. N-terminal fusion peptide encodes an ATG translation initiation codon, six histidine residues in series that functions as a metal binding domain in the translated protein, the bacteriophage T7 gene 10 translation enhancer, the Xpress epitope, and an enterokinase cleavage recognition sequence that allows removal of the fusion peptide from the translated protein. The ampicillin resistance gene allows for selection of *E. coli* containing the plasmid at a reasonable copy number to survive the ampicillin selection.

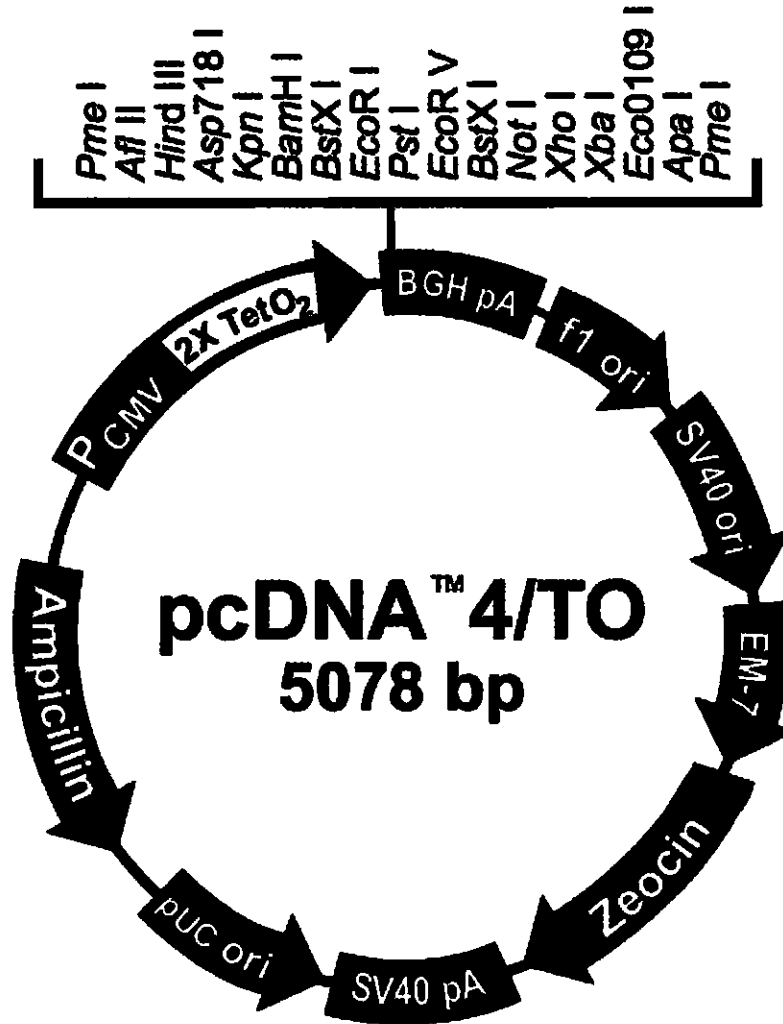


Figure 2.2. pcDNA 4/TO vector map.

This plasmid contains the control elements from the bacterial tetracycline resistance operon to effectively repress, and de-repress, transcription of genes cloned into the multiple cloning site. When stably integrated into the target cell line, which already contains the genomically integrated pcDNA6/TR, repression of the gene of interest can be alleviated with the addition of tetracycline (1 μ g/ml 16 h). The mammalian drug resistance gene for Zeocin allows for effective selection of genomic integration. The ampicillin resistance gene allows for selection of *E.coli* containing the plasmid at a reasonable copy number to survive the ampicillin selection.

Design of PCR primers. Primer sequences were designed for expression of TRPA1 carboxyl (C) and amino (N) terminals and CKM in the pTrcHisB vector and CKM, CKMT1B and CKMT2 in the pcDNA 4/TO vector. Both sense and anti-sense primers were designed based on the human cDNA sequences shown in Table 2.2 (Invitrogen, TX). Restriction enzymes (NEB) were selected that digest only at one site within the multiple cloning site of the selected vector and did not contain restriction sites within the selected insert sequence. Restriction site sequences for the selected restriction enzymes (underlined) were introduced to the primers. All primers contained a six base pair overhang at the start of the sequence and all reverse primer sequences are reverse complemented to the cDNA target sequence and include a stop codon sequence directly after the restriction enzyme sequence. Primers for the pcDNA 4/TO vector contain a V5-epitope tag sequence in **bold print** and forward primers for the pTrcHisB vector contain an extra base pair that was added after the restriction enzyme site to keep the insert DNA in frame with the vector sequence.

Table 2.2. PCR primers.

Primer Name	Melting Temp. °C	Restriction Enzyme	Nucleotide Sequence 5' to 3'
pTrcHisB Vector			
TRPA1 N-term	77.4	XhoI	AAATGTCTCGAGAATGAAGCGCAGCCTGAGGAAGATGTGG
TRPA1 N-term	60.9	KpnI	AAATGTGGTACCTTAATGATTGAGAAGCTCTATGC G
TRPA1 C-term	62.4	XhoI	AAATGTCTCGAGAGTCCAGAAACATGCATCATTG AAGAGGATAGCTATGCAGGTG
TRPA1 C-term	69.8	KpnI	AAATGTGGTACCCTAAGGCTCAAGATGGTGTGTTT TTGC
CKM	69.4	Xho I	AAATGTCTCGAGAATGCCATTCGGTAACACCCAC AACAAGTTCAAGCTGAATTACAAGCCTGAGGAGG AGTACCCC
CKM	69.6	Kpn I	AAATGTGGTACCCTACTTCTGGGCGGGGATCATGT CGTCAATGGACTGGCCTTCTCCAACCTTCTCTC
pcDNA 4/TO Vector			
CKM	64.0	Kpn I	AAATGCGGTAACATGCCATTCGGTAACACCCACA ACAAGTTCAAG
CKM	76.0	Not I	GCATTTGCGGCCGCCTACGTAGAATCGAGACCG AGGAGAGGGTTAGGGATAGGCTTACCCTTCTGG GCGGGGATCATGTCGTC
CKMT1 B	66.8	Kpn I	AAATGCGGTAACATGGCTGGTCCCTTCTCCCGTCT GCTG
CKMT1 B	75.4	Not I	GCATTTGCGGCCGCCTACGTAGAATCGAGACCG AGGAGAGGGTTAGGGATAGGCTTACCATGCTTG GTGTGGATGACAGGTGTGGG
CKMT2	66.4	Afl II	AAATGCCTTAAGATGGCCAGTATCTTTTCTAAGTT GCTAACTGGCCGCAATGCTTCTCTG
CKMT2	73.8	Xho I	GCATTTCTCGAGCTACGTAGAATCGAGACCGAG GAGAGGGTTAGGGATAGGCTTACCCTTTTGGCC AAACCTGAGGCAGAGGGGG

PCR. PCR reactions were performed using the “AccuPrime™ Pfx SuperMix” (Invitrogen, CA.), comprising 22 U/ml *Thermococcus* species KOD thermostable polymerase complexed with anti-KOD antibodies, 66 mM TrisSO₄ pH 8.4, 30.8 mM (NH₄)₂SO₄, 11 mM KCl, 1.1 mM MgSO₄, 330 μM dNTPs. Reaction schemes optimized for specific primer pairs are shown below.

V5-tagged CKM (1146bp), CKMT1B (1255bp) and CKMT2 (1260bp). Hot start PCR was held at 95°C for 5 min followed by 35 cycles of denaturation (95°C, 1 min), annealing (58°C, 30 sec), and extension (68°C, 1 min 20 sec), then a final elongation period (68°C, 2 min 40 sec) and held upon completion at 14°C.

TRPA1 C-Terminal (462bp). Hot start PCR was held at 95°C for 5 min followed by 35 cycles of denaturation (95°C, 1 min), annealing (57°C, 30 sec), and extension (68°C, 1 min), then a final elongation period (68°C, 2 min) and held upon completion at 14°C.

TRPA1 N-Terminal (2100bp). Hot start PCR was held at 95°C for 5 min followed by 35 cycles of denaturation (95°C, 1 min), annealing (55°C, 30 sec), and extension (68°C, 2 min), then a final elongation period (68°C, 4 min 20 sec) and held upon completion at 14°C.

CKM (1146bp). Hot start PCR was held at 95°C for 5 min followed by 35 cycles of denaturation (95°C, 1 min), annealing (55°C, 30 sec), and extension (68°C, 1.5 min), then a final elongation period (68°C, 3 min) and held upon completion at 14°C.

Gel electrophoresis of DNA and band excision. Agarose gel electrophoresis was performed using 1% agarose in TAE buffer (comprising 40 mM Tris, 20 mM acetic acid, and 2 mM EDTA pH 8.3). Samples were loaded in a 1X final concentration of 10X

DNA loading buffer comprising bromophenol blue (0.25% w/v), xylene cyanol (0.25% w/v), Ficoll 400 (20% w/v), EDTA (0.1 M, pH 8.0), and SDS (1% w/v), and electrophoresed at 9-15 V/cm for the time needed to achieve adequate resolution. DNA ladders spanning the 100 bp –10 kb range (New England Biolabs, MA) were used to determine the size of visible fragments. DNA gels were visualized on a ChemiDoc system (BioRad), using ethidium bromide (0.5 µg/ml final). Bands were excised by a clean scalpel and extracted using the QIAquick Gel Extraction Kit.

Digest and Ligation. The insert and vector were digested with 1 µl of each of the restriction enzymes (specified in the primer pairs) in the recommended reaction buffer (NEB) supplemented with 100 µg/ml BSA for 2 hr at 37°C. One microliter of calf intestinal phosphatase (CIP, 10 U, Invitrogen) was added into the insert reaction for the last 30 min. Prior to the ligation reaction, the digested vector was confirmed by agarose gel electrophoresis and then extracted from the gel using the QIAquick Gel Extraction Kit (Qiagen, CA). The insert was purified using the QIAquick PCR purification Kit (Qiagen). Ligation reactions occurred in a 50 µl reaction volume, containing 5 µl T4 DNA ligase buffer (10X, NEB), 1 µl T4 DNA ligase (400 U, NEB), 100 ng of target vector, plus a one or three times, molar equivalent of the target insert (or water in the control reaction). Reaction volume was completed with autoclaved water purified by Millipore RO system (Millipore, MA). The reaction mixture was incubated at 16°C for 16-72 hr.

Transformation and bacterial culture. Competent XL-10-Gold Ultracompetent cells (Stratagene, TX) or One Shot TOP10 competent cells (Invitrogen) were thawed on wet

ice for no longer than 10 min. Two microliters of beta-mercaptoethanol were added to the cells and incubated for 10 min. Next, four microliters of ligation reaction products were added, mixed gently with pipette tip and left to incubate for 30 min on wet ice. The mixture was then heat-shocked at 42°C for 45 sec, 500 µl of pre-warmed (37°C) SOC media (Invitrogen) was added, and the culture incubated for 1 hr at 37°C, while shaking at 225 rpm in a C25 incubator shaker (New Brunswick Scientific, NJ). Culture volumes of 100 µl, and 400 µl, were plated onto, two separate LB Miller agar (LB, Fisher Scientific, PA) plates containing 50 µg/ml Ampicillin. These plates were then incubated for 16-18 hr at 37°C. Colonies from these plates were then picked and grown in 5 ml of LB broth containing 50 µg/ml Ampicillin. The QIAprep 8 plus Turbo Miniprep Kit was used for purification of up to 20 µg plasmid DNA from 5 ml bacterial cultures

Screening of constructs for presence of insert. Miniprep samples were digested, as described previously, for 2 hr at 37°C. Digestion was confirmed by agarose gel electrophoresis. Positive colonies were determined to have correct inserts of the correct size by comparison with a 1 kb DNA ladder.

Retransformation and bacterial culture. Competent Library efficiency DH5α (Invitrogen) or XL-10-Gold Ultracompetent (Stratagene) cells were thawed on wet ice for no longer than 10 min. Two microlitres of positive miniprep products were added and mixed gently with pipette tip. The mix was left to incubate for 30 min on wet ice. The mixture was then heat-shocked at 42°C for 45 sec, 500 µl of SOC media (Invitrogen) pre-warmed to 37°C was added, and the culture incubated for 1 hr at 37°C, while shaking at 225 rpm. LB agar plates containing 50 µg/ml Ampicillin were used to plate 20-50 µl of

the cultures. These plates were then incubated for 16 to 18 hr at 37°C. Colonies from these plates were then picked and grown in 200 ml of LB broth containing 50 µg/ml Ampicillin. Cells were harvested by centrifuging at 6000x g for 20 min in an Avanti J-25 centrifuge (Beckman Coulter, CA). The QIAfilter Plasmid Maxi Kit (Qiagen) was used for purification of up to 500 µg ultrapure plasmid DNA, from 200 ml bacterial cultures. DNA concentration and purity were determined by measurement of O.D. at 260 nm and 280 nm on a Beckman DU650 Spectrophotometer (Beckman Coulter).

DNA sequencing. All cDNA inserts were validated by full-length sequencing, which was performed at the Advanced Studies in Genomics, Proteomics and Bioinformatics Facility, at the University of Hawaii (<http://cgpbr.hawaii.edu/>) on a fee-for-service basis. Typically, 200-300 ng plasmid DNA and 3.2 pmol primer, was provided for analysis using Applied Biosystems BigDye terminator chemistry on ABI 3730XL capillary-based DNA sequencers. Sequencing reactions were performed in both, forward and reverse, directions, and analyzed using FinchTV 1.3.1 (Geospiza Inc., WA), AssemblyLign (Accelrys, CA) and MacVector software (Accelrys) for identification.

Table 2.3. Sequencing primers.

pTrcHisB		
Fwd		5'- GAGGTATATATTAATGTATCG -3'
Rev		5'- GATTTAATCTGTATCAGG -3'
PcDNA4/TO		
Fwd		5'- GTCAGATCGCCTGGAGACGCC -3'
Rev		5'- AGGAAAGGACAGTGGGAGTG -3'
TRPA1		
F4	351-369	5'- TCTCAGCAGAGGAGCAAAC -3'
F7	518-539	5'- GCACCACAAATAATAGCGAAGC -3'
F9	877-895	5'- TCGTCCTATTCTGGTAGCG -3'
F11	907-925	5'- AACACAACCGATGGATGTC -3'
F14	1084-1102	5'- CTCTCTAAAGGTGCCCAAG -3'
F17	1402-1423	5'- GACATAAGTGATACGAGGCTTC -3'
F25	1719-1738	5'- CATAGTCCTGAACAAGCAGC -3'
F32	2038-2056	5'- TATGAACCGCTTACAGCCC -3'
F36	2225-2243	5'- CAGGAATGGCTTTCAACTC -3'
F37	2424-2443	5'- ATGGATTATCTACACGACGG -3'
F40	2866-2885	5'- CTTATTGGTTTGGCAGTTGG -3'
F49	3302-3325	5'- GCAGATGGAATACTGTGTTGAGAG -3'
R50	73-55	5'- CATCCTCATAGACAACGCC -3'
R62	1034-1015	5'- GGAGAGCGTCCTTCAGAATC -3'
R67	1239-1216	5'- CCCATCGTTGTCTTCATCCATTAC -3'
R68	1402-1383	5'- CTTGTAGGAGCCTCTGACAG -3'
R92	2905-2886	5'- TCTGGACCTCAGCAATGTCG -3'
R94	2996-2978	5'- TCCACTTTGCGTAGAAACC -3'
CKM		
F20	306-325	5'- CACTGACAAGCACAAGACTG -3'
R26	645-633	5'- TGGCATCTGGCACAATGAC -3'
R66	1046-1027	5'- TGTTCTACTTCGGACGAGCC -3'
CKMT1B		
F6	348-369	5'- GGTATTTGCTGACCTGTTTGAC -3'
R60	947-926	5'- CAGGTCAAGATGTATCCCAAAC -3'
CKMT2		
F10	344-363	5'- CCTATGAGGTGTTTGCTGAC -3'
R64	957-939	5'- CGAAGGACAGGTCAAATG -3'

2.3 Protein Expression and Biochemistry

Expression and Extracton of His-Tagged Proteins. Competent BL21-A1 One Shot cells (Invitrogen) were thawed on wet ice for no longer than 10 min. Two microlitres of positive miniprep products were added and mixed gently with pipette tip. The mix was left to incubate for 30 min on wet ice. The mixture was then heat-shocked at 42°C for 45 sec, 250 µl of pre-warmed (37°C) SOC media was added, and the culture incubated for 1 hr at 37°C, while shaking at 225 rpm. LB agar plates containing 50 µg/ml ampicillin were used to plate 20-50 µl of the cultures. These plates were then incubated for 16 to 18 hr at 37°C. Colonies from these plates were then picked and incubated in 20 ml of LB broth containing 50 µg/ml ampicillin for 12-16 hr at 37°C, while shaking at 225 rpm. Cultures were then transferred into 400 ml LB with ampicillin (50 µg/ml) in a ratio of 1:80 followed by incubation at 37°C, while shaking at 225rpm until OD₆₀₀ reaches 0.6. After removal of 1 ml culture as control, IPTG was added to a final concentration of 0.4 mM to induce expression. After an incubation and growth to OD₆₀₀ of 0.8, cells were harvested by centrifuge at 6000 x g for 30 min in an Avanti JLA-10.5 centrifuge (Beckman). The BL-21 pellets were resuspended in 40 ml 1X binding buffer from the Novagen His-Bind Kit (EMD Chemicals Inc., CA). The mammalian protease inhibitor cocktail (1 µg/ml Sigma-Aldrich, MO) was to prevent protein degradation. The homogenous lysate was sonicated using a VCX600 sonicator (Sonics & Materials Inc.) at 50% power for 30 sec at 4°C. The sonication was repeated eight times, with 1 min on ice between intervals. The lysate was then frozen at -80°C.

Purification of His-Tagged Proteins by Affinity Chromatography and Dialysis.

Protein purification was performed using the His-Bind Resin Chromatography protocol included in the Novagen His-bind protein purification kit (EMD Chemicals Inc., CA). The lysate was thawed in cool running water, iced, then centrifuged at 14,000 x g in an Avanti J-25 centrifuge (Beckman) centrifuge for 20 min. The supernatant was filtered through a 0.2 µm syringe filter in order to further reduce viscosity. Two milliliters of 50% His-Bind resin slurry was added to a sealed column and allowed to settle by gravity flow. After all beads settled down, the seal was removed to allow elution of the resin suspension solution. This was followed by application of 3 ml sterile water, 5 ml charge buffer and 3 ml binding buffer to charge Ni²⁺ on the beads. The column was loaded with the filtered protein lysate and then washed with 10 ml binding buffer and 6 ml wash buffer. Finally, 6 ml of elution buffer was applied to the column and collected as six 1 ml aliquots. All buffers and supernatants were passed through the column by gravity flow.

Protein Quantification. Where indicated, protein samples were matched for total protein levels based on a colorimetric protein determination assay. The D_c Protein Determination Kit™ (BioRad, CA) was used. After cell lysis, triplicate samples of 5 µl were removed from each lysate and transferred to a 96 well microtitre plate. According to the Manufacturer's instructions 25 µl per well of reagent A' was added to each well followed by addition of 200 µl of reagent S (substrate) and incubation for 10 min at room temperature. Color development was read at 710 nm in a Benchmark Plus (BioRad) plate reader. Where absolute protein levels were calculated, this was done in relation to a

standard curve generated using serial dilutions of bovine serum albumin (BSA) in 1X PBS.

Proteins concentration was also determined by UV absorption (260-280 nm) using the following equation: $[\text{Protein}] \text{ (mg/mL)} = 1.55 \cdot A_{280} - 0.76 \cdot A_{260}$

Protein Determination by SDS PAGE. The polyacrylamide resolving gels used consisted of 10-15% (as indicated in the figure legends) 30% acrylamide/bis solution 37.5:1 (2.6% c, BioRad) with 1% (v/v) SDS. Electrophoresis was performed at 50-60 volts for 16-20 hr in buffer containing: 0.192 M glycine, 25 mM Tris-Base pH 8.8, and 0.05% SDS. The All Blue Precision Plus Protein standard (BioRad), was used to approximate the molecular weight of proteins separated by SDS-PAGE.

Coomassie Blue Staining. Gels were immediately soaked in Coomassie staining buffer for 1-2 hr after removal from the gel apparatus, and were then destained in destaining buffer until clear bands could be seen. Composition of staining and destaining buffer are as follows: 100 ml of Coomassie staining buffer contained 0.1% (w/v) Coomassie brilliant blue R-250, 10% (v/v) glacial acetic acid, and 45% (v/v) methanol. Destaining buffer was 10% (v/v) glacial acetic acid and 10% (v/v) methanol.

Western blot analysis. Resolved proteins were transferred from polyacrylamide gels to polyvinylidene fluoride (PVDF) membranes (activated for 30 sec in methanol) by electroblotting in transfer buffer (192 mM Glycine and 25 mM Tris-Base pH 8.8) at 1.4 A for 200 min at 4 °C. Then, membranes were blocked by non-fat milk solution (5% w/v in PBS) at room temperature for 1 hr with gentle shaking. Primary antibodies were dissolved in PBS with 0.05% (w/v) Tween-20, 0.02% (w/v) sodium azide, and 0.5%

(w/v) BSA, and incubated with the membrane at 4°C overnight. Secondary HRP-conjugated IgG antibodies were dissolved in TTBS (15 mM Tris, 0.15M NaCl and 0.1% w/v Tween-20) with 0.5% non-fat milk and incubated with membrane at room temperature for 1 hr. Washes between incubations were performed in TTBS for 5 min and repeated four times. Finally, membranes were exposed to ECL plus solution (GE Healthcare, NJ) for 4 min and wrapped in plastic wrap. Signals were visualized using Kodak X-OMAT LS scientific imaging film on a Kodak X-OMAT 2000A processor.

Stripping and Re-probing of Western Blots. Blots were stripped by shaking at 50°C for 20 min in 100 mM 2-mercaptoethanol, 2% SDS, 63.5 mM Tris-HCL pH 6.7. Membranes were then washed twice for 10 min each in TTBS at room temperature then blocked and probed as described above.

Table 2.4. Antibodies.

Epitope	Animal Source	Company Source	Catalog Number	Dilution of Stock used on Western
TRPA1/ANKTM1	Rabbit Polyclonal	Synthesized, Bethyl Laboratories, Montgomery, TX	na	1:1000 or 1:500 (Co-IP)
CK-BB	Mouse Monoclonal	Fitzgerald Industries International Inc. Concord, MA	10-C42	1:750
CK-MM	Mouse Monoclonal	Fitzgerald Industries International Inc. Concord, MA	10-C41	1:750
Cyclin B1	Mouse Monoclonal	Cell Signaling Technology, Inc. Danvers, MA	4135	1:1500
Flag M2	Mouse Monoclonal	Sigma-Aldrich Co. St. Louis, MO	F 3165	1:5000
GRB2, clone 3F2	Mouse Monoclonal	Upstate Cell Signaling Solutions Lake Placid, NY	05-372	1:1000
6X His tag	Mouse Monoclonal	Abcam Inc. Cambridge, MA	ab18184	1:500
E1 α subunit of PDH	Mouse Monoclonal	Molecular Probes Inc. Eugene, OR	A-21323	1:1000
PMP70	Rabbit Polyclonal	Abcam Inc. Cambridge, MA	ab3421	1:1000
VDAC1/Porin	Mouse Monoclonal	Abcam Inc. Cambridge, MA	ab14734	1:1000
V5-Tag	Mouse Monoclonal	AbD Serotec, MorphoSys UK Ltd, Oxford, UK	MCA1360	1:2000

Dialysis. To eliminate the Tris and reduce the salt (500 mM) from the eluted sample, His-tagged proteins were dialyzed twice for 2-4 hr against 1 L each of 0.1 M MOPS pH 7.5 (with 80 mM NaCl for the AFC-N terminal samples) using slide-a-lyzer dialysis cassettes with a molecular weight cut off of 3500 daltons (Pierce, Illinois).

2.4 Cell Biology

Maintenance of cell culture. The HEK293Trex cell line was maintained in Dulbecco's Modification of Eagle's Medium (DMEM) (Mediatech Inc, VA) supplemented with 10% fetal bovine serum and 2 mM glutamine in humidified 5% CO₂ at 37°C. The AFC cell line was maintained in DMEM supplemented with 10% fetal bovine serum, 2 mM glutamine 200 ug/ml Hygromycin and 5 ug/ml blasticidin in humidified 5% CO₂ at 37°C. All other cell lines were maintained in appropriate culture media under the same incubation conditions.

Sub-cellular Fractionation. Two different protocols were used to obtain sub-cellular fractions from HEK cells. Details of both protocols are provided below. The 1X lysis buffer contains; 50 mM Hepes pH 7.4, 20 mM NaF, 10 mM iodoacetamide pH 7.4 and the reducing sample buffer (RSB) contains; 20% (v/v) glycerol, 62.5 mM Tris-HCl pH 6.8, 0.05% (w/v) bromophenol blue, 2 mM 2mercaptoethanol.

Protocol 1. HEK293Trex cells were harvested from 20- 15 cm plates, spun 5 min at 200 x g at RT, re-suspended in 10 ml 1X PBS, spun 10 min at 200 x g at RT then re-suspended in 3 ml of ice cold IBc buffer (100 M Tris-MOPS, 10 mM EGTA Tris, 200 mM sucrose, pH 7.4) and incubated 10-20 min on ice. Cells were homogenized by 30-40 strokes with a Teflon pestle, a sample of the total lysate was taken (Total Lysate), and then the lysate was spun for 10 min at 600 x g at 4°C. A sample of the nuclear pellet (Nuclear) was taken and the supernatant was spun 10 min at 7,000 x g at 4°C. Supernatant containing the plasma membrane and endoplasmic reticulum was removed and a sample was taken. The pellet was washed in 300 µl ice cold IBc then transferred to

a 1.5 ml tube and spun 10 min at 7,000 x g at 4°C. Supernatant was removed and the pellet containing the mitochondria, lysosomes and peroxisomes was resuspended in residual buffer. Samples were lysed in high salt lysis buffer (1X lysis buffer with 250 mM NaCl) 30 min on ice, acetone precipitated (added acetone 1.4 times the sample volume, spun 12,000 x g for 5 min at 4°C) then resuspended in RSB.

Protocol 2. HEK293TRex cells were harvested from 20- 15 cm plates, spun 5 min at 200 x g at RT, re-suspended in 10 ml 1X PBS, spun 10 min at 200 x g at RT then re-suspended in 3 ml ice cold hypotonic buffer (10 mM NaCl, 1.5 mM MgCl₂, 10 mM Tris pH 7.5) and incubated 10-20 min on ice. Cells were homogenized by 30-40 strokes with a Teflon pestle and MS buffer (525 mM mannitol, 175 mM sucrose, 12.5 mM Tris pH 7.5, 2.5 mM EDTA pH 7.5) was added to 15 ml total volume. A sample of the Total Lysate was taken then the lysate was spun 10 min at 1,300 x g at 4°C. A sample of the nuclear pellet was taken, then nuclear and total lysate samples were lysed 30 min on ice in lysis buffer B (1X lysis buffer with 25 mM NaCl, 2% Triton and protease inhibitors), acetone precipitated and resuspended in RSB.

The supernatant was spun 10 min at 5,500 x g at 4°C. The mitochondrial pellet was resuspended in 1.5 ml 0.3 M sucrose, then layered on top of 10 ml 1.6 M sucrose and spun 1 hr at 100,000 x g in a SW41Ti ultracentrifuge rotor. Mitochondria were removed after centrifugation and lysed 20 min on ice in lysis buffer A (1X lysis buffer with 2% Triton and protease inhibitors), acetone precipitated and resuspended in RSB.

The supernatant was spun 30 min at 15,000 x g. The resulting pellet was resuspended in 2 ml sucrose diluent, layered on a sucrose gradient (1.09-1.25 M in 1 mM

EDTA, 10 mM TRIS/HCl pH 7.4, 1 mM PMSF) and spun for 1 hr at 100,000 x g. The resulting protein bands containing the lysosomes and peroxisomes were extracted and RSB was added to a 1X final concentration. The supernatant was spun 1 hr at 100,000 x g and the resulting pellet containing the endoplasmic reticulum was lysed in Lysis buffer C (1X lysis buffer with 1% Triton X-100 and mammalian protease inhibitor cocktail (Invitrogen), acetone precipitated, and resuspended in RSB.

Sub-cellular samples were separated by SDS-PAGE and visualized by western blot analysis. Details regarding the concentrations of antibodies used are provided in Table 2.4.

Transient Transfection. HEK293TRex cells (Invitrogen, Carlsbad, CA) were seeded and grown until 50% confluent. All cDNA was purified using a QIAfilter Plasmid Maxi Kit (Qiagen, Valencia, CA). The cDNA quality was measured using a spectrophotometer and used in transfection only if O.D. 260/280 > 1.7. HEK293 cells were transiently transfected using reagent LT1 (Mirus, Madison, WI). Serum free DMEM (150 μ l) and LT1 reagent (10 μ l) were mixed together then vortexed for 30 sec. The mixture was then left at room temperature for 15 min. After 15 min, the cDNA was added to the mixture and mixed gently. After 15 min at RT, the mixture was added to the cells in a drop-wise manner while swirling the plate. The cells were then placed in a humidified 5% CO₂ incubator for 48-72 hr. Construct-expression was induced by addition of 1 μ l per ml of tetracycline for 16-20 hr.

Total lysate preparation. For preparation of total protein, cells were pelleted (2,000 x g, 2 min) and washed once in room temperature PBS. Approximately 1 x 10⁷ cells were

lysed (ice/30 min) in 350 μ l of lysis buffer (50 mM Hepes pH 7.4, 75 mM NaCl, 20 mM NaF, 10 mM iodoacetamide, 0.5% (w/v) Triton X100, 1 mM PMSF (phenylmethylsulfonyl fluoride), 500 μ g/ml Aprotinin, 1.0 mg/ml Leupeptin and 2.0 mg/ml chymostatin). Lysates were then clarified (10,000 x g, 5 minutes). Lysates were precipitated by addition of 1.4 times the sample volume of acetone for one or more hours at -20°C. Lysates were pelleted (10,000 x g, 1 minute) and boiled in reducing sample buffer (RSB; 20% (v/v) glycerol, 62.5mM Tris-HCL pH6.8, 0.05% (w/v) bromophenol blue, 2mM 2mercapto-ethanol).

Co-Immunoprecipitation. Cells were pelleted (2,000 x g, 2 minutes) and washed once in room temperature PBS. Approximately 1×10^7 cells were lysed (ice/30 min) in 350 μ l of lysis buffer (50 mM Hepes pH 7.4, 75 mM NaCl, 20 mM NaF, 10 mM iodoacetamide, 0.5% (w/v) Triton X100, 1 mM PMSF (phenylmethylsulfonyl fluoride), 500 μ g/ml Aprotinin, 1.0 mg/ml Leupeptin and 2.0 mg/ml chymostatin). Lysates were then clarified (10,000 x g, 5 min). For immunoprecipitation, supernatants were rotated (4°C / 2 hr) with the indicated antibody, followed by addition of Protein A agarose diluted to 50% in lysis buffer (20 μ l, Sigma). Samples were boiled in RSB and stored at 4°C.

CHAPTER 3: TRPA1 INTERACTS WITH HUMAN CREATINE KINASES

3.1 Introduction

Initial interaction trap analysis, obtained via the Sos recruitment system assay (SRS), provided an extensive set of potential binding partners for the TRPA1 cytoplasmic tail. One of these was the rat brain specific isotype of creatine kinase (CKB). (Stokes, unpublished data) The potential interaction of CKB with TRPA1 suggested that CKB might be involved in the regulation of TRPA1 channel activity. Results presented in this chapter demonstrate the co-immunoprecipitation of stably over-expressed FLAG-TRPA1 and transiently over-expressed V5-epitope-tagged CKB proteins in a HEK cell line (AFC cells).

Confirmation of this interaction suggested that TRPA1 might also interact with the other three isoforms of creatine kinase. This idea was supported by preliminary electrophysiological data (Figure 1.3) that showed the inhibition of the characteristic TRPA1 current in TRPA1 over-expressing HEK293TREx cells (AFC cells, see Materials and Methods) when CKM was added to the internal bath solution. Since the potential binding partners for the SRS assay originated from a rat brain library, large amounts of the creatine kinase isoforms that are not brain specific would not exist. Results from the additional co-immunoprecipitation experiments performed in AFC cells demonstrate interactions between stably over-expressed human TRPA1 and transiently over-expressed isoforms of human creatine kinase proteins, found in muscle (M) and mitochondria (MT1B and MT2).

3.2 Results

Confirmation of the CKB-TRPA1 interaction in a human cell line.

The interaction between full length over-expressed TRPA1 and human CKB was validated in TRPA1-FLAG-HEK293TREx (AFC) cells. To achieve this, 0.5 -2 μ g of the V5-CKB pcDNA4/TO construct (see Materials and Methods) was transiently lipid transfected into AFC cells induced to over-express FLAG-TRPA1. Proteins from the lysates of these cells were immunoprecipitated with the anti-FLAG antibody. Immuno-complexes were separated by SDS-PAGE and proteins were detected on a western blot with FLAG and V5 antibodies.

The results in Figure 3.1 show that the FLAG antibody detected a protein with a molecular weight of 127 kDa corresponding to FLAG-TRPA1 protein (predicted molecular weight 127 kDa) and another protein of higher molecular weight (>250 kDa). The V5 antibody detected V5-CKB co-immunoprecipitated protein (predicted molecular weight 43 kDa). Relative amounts of V5-CKB protein detected on the western blot appeared to correspond to the amount of the corresponding construct transformed into the cells. The heavy (50 kDa) and light (25 kDa) chains FLAG antibody are present in all blots visualized with mouse-specific secondary antibodies (the same species as the FLAG antibody used for the immunoprecipitation).

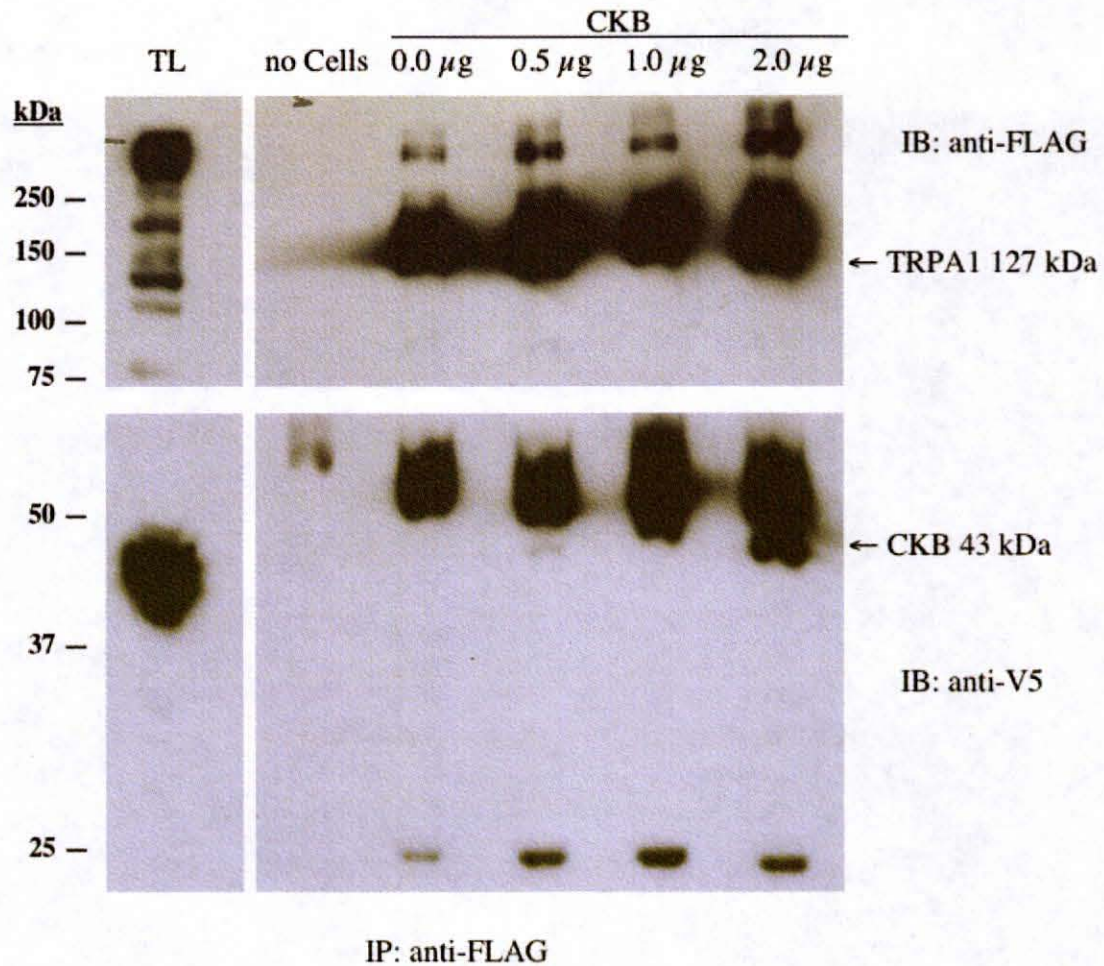


Figure 3.1. Western blot showing co-immunoprecipitation of V5-CKB by FLAG-TRPA1.

Left panel contains total lysate from FLAG-TRPA1 over-expressing HEK293TRex (AFC) cells lipofected with 6 μ g V5-CKB construct. Right panel contains: FLAG antibody immunoprecipitation without cells and from AFC cells transiently over-expressing V5-CKB. Lipofection amounts of V5-CKB are 0 μ g, 0.5 μ g, 1.0 μ g and 2 μ g. Immunocomplexes were resolved by SDS-10% PAGE and western-blotted with V5 and TRPA1 antibodies. The predicted molecular weight of TRPA1 is 127 kDa and CKB is 43 kDa. FLAG antibody heavy and light chain proteins are visible at 50 kDa and 25 kDa.

Production of V5-tagged creatine kinase constructs in the pcDNA4/TO vector

Constructs of CKM, CKMT1B and CKMT2 with a C-terminal V5-epitope tag were amplified and subcloned into the pcDNA4/TO vector. To begin, PCR primers were designed to target the cDNA sequences for the three CKs and incorporate a V5-tag at the carboxyl terminus of each sequence. PCR primer sequences are presented in Table 2.2 followed by PCR reaction conditions (see materials and methods). Successful amplification of target sequences by PCR is shown in Figure 3.2.

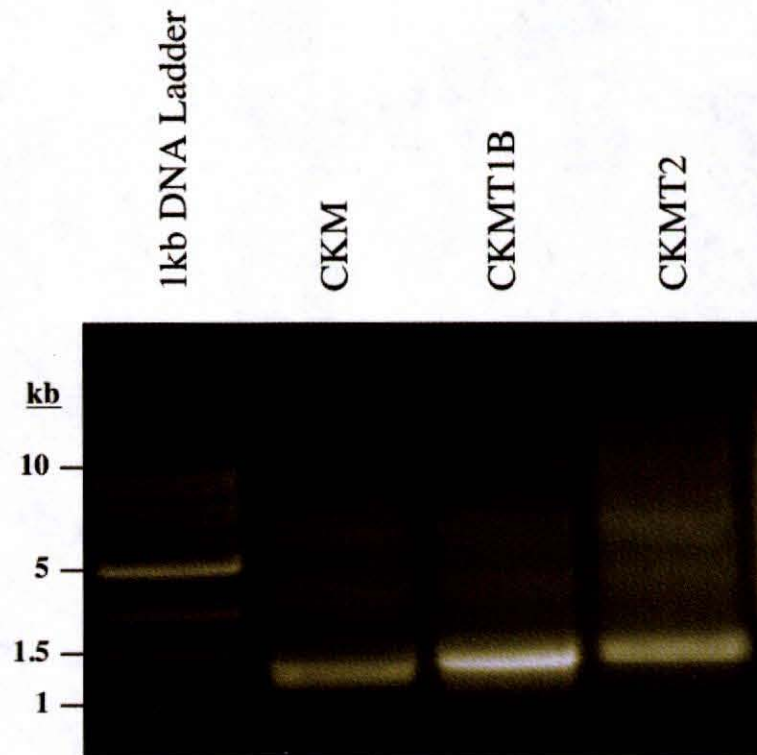


Figure 3.2. V5-tagged creatine kinase PCR products.

CKM (1146 bp) CKMT1B (1255 bp) and CKMT2 (1260 bp) cDNA sequences with an C-terminal V5-epitope tag sequence were amplified by PCR and electrophoresed on a 1% agarose gel with ethidium bromide.

Target sequences were then subcloned into a tetracycline-inducible pcDNA4/TO expression vector (Figure 2.2). The pcDNA4/TO expression vector is designed for stable expression of a gene of interest in mammalian cells. When stably integrated into a cell line containing genomically integrated pcDNA6/TR, such as the HEK293TRex cell line, repression of the gene of interest can be alleviated with the addition of tetracycline. Target sequences were subcloned into the pcDNA4/TO using the following restriction

enzymes: Kpn I and Not I (CKM and CKMT1B) and Xho I and Afl II (CKMT2). An overview of the subcloning strategy is shown in Figure 3.3.

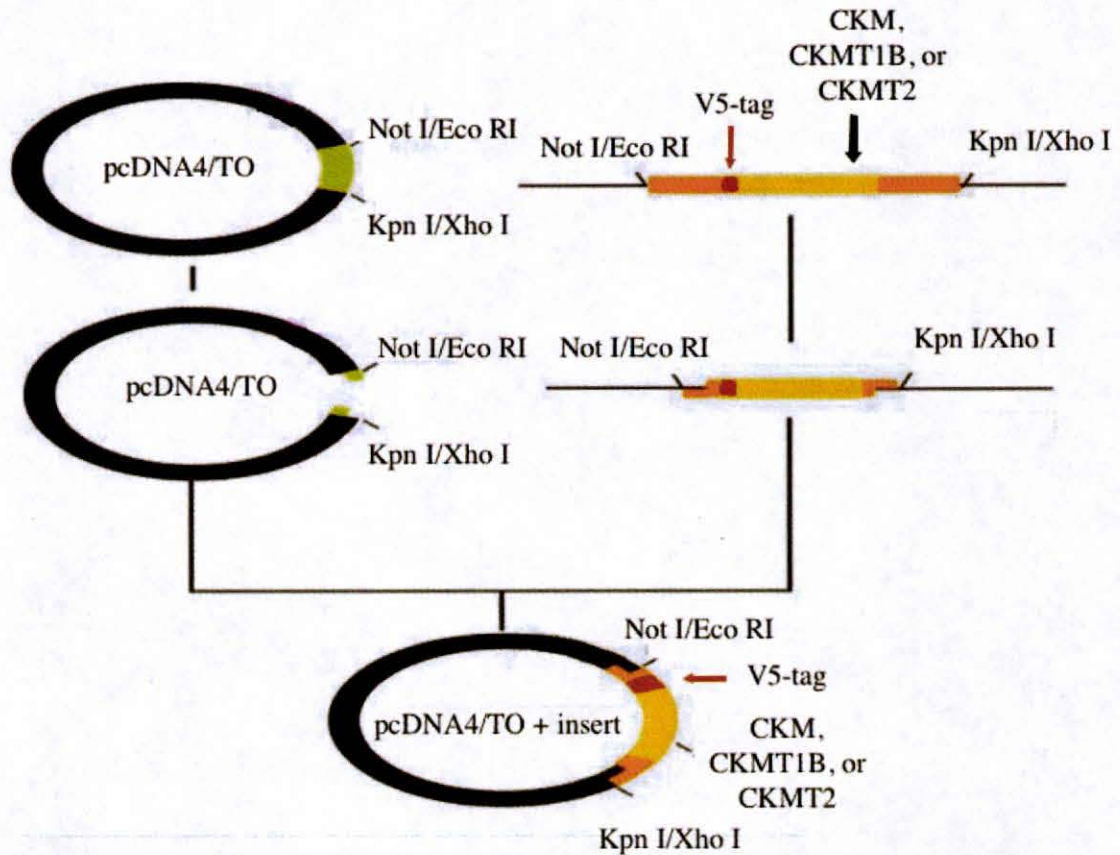


Figure 3.3. CK-V5 sub-cloning strategy.

Insert DNA was amplified by PCR with primers that confer Eco RI and Xho I or Not I and Kpn I restriction sites. The PCR products and pcDNA4/TO vector were digested with both restriction enzymes, and then ligated together. These constructs were transformed into, expressed in, and isolated from competent *E. coli*.

The results from an enzymatic digest of the initial subcloning miniprep products are shown in Figures 3.4 and 3.5. Constructs digested with both restriction enzymes contain a vector band at approximately 5 kb and insert bands of approximately 1.2 kb.

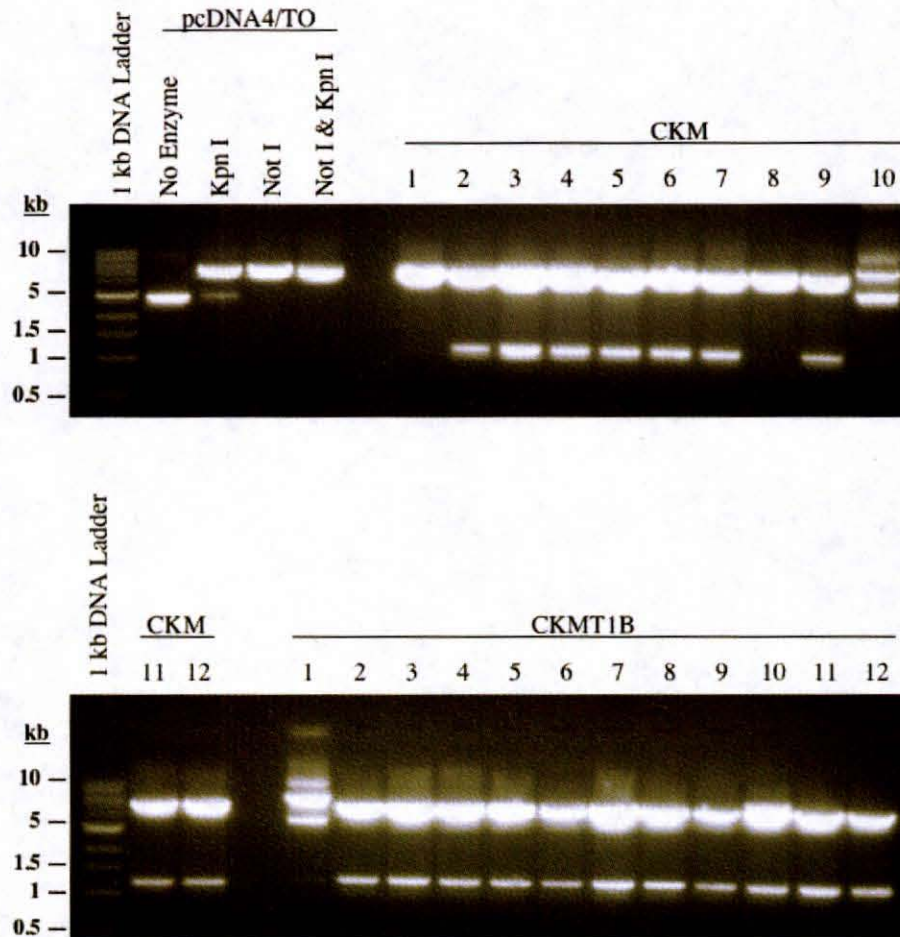


Figure 3.4. Restriction enzyme digested CKM- and CKMT1B-pcDNA4/TO constructs.

Restriction enzyme digested CKM- and CKMT1B-pcDNA4/TO constructs electrophoresed on a 1% agarose gel with ethidium bromide. Digestion was performed as indicated for 2 hr at 37°C. Controls include; undigested pcDNA4/TO vector, vector digested with only Kpn I or Not I and vector digested with Kpn I and Not I. Successful transformation is indicated by digested miniprep samples (1-12) containing both vector about 5 kb and insert about 1.2 kb.

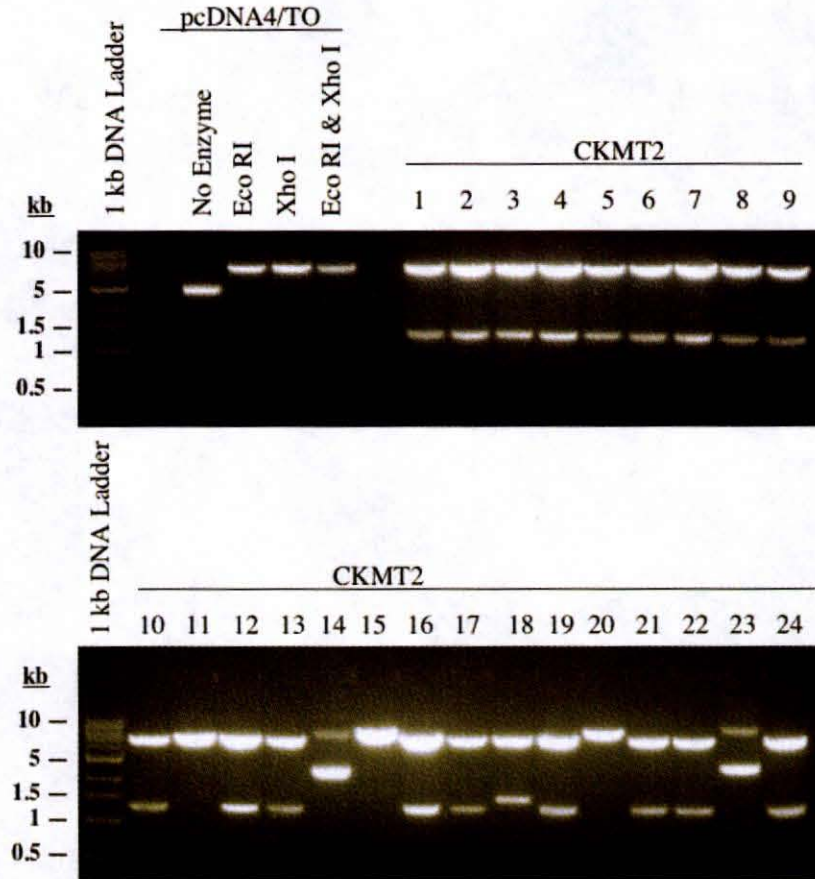


Figure 3.5. Restriction enzyme digested CKMT2-pcDNA4/TO constructs.

Restriction enzyme digested CKMT2-pcDNA4/TO constructs electrophoresed on a 1% agarose gel with ethidium bromide. Digestion was performed as indicated for 2 hr at 37°C. Controls include; undigested pcDNA4/TO vector, vector with Eco RI, vector with Xho I and vector with Eco RI and Xho I. Successful transformation is indicated by digested mini-prep samples (1-24) containing both vector about 5 kb and insert about 1.2 kb.

Clones that tested positive for the expression of inserted target sequences were selected and re-amplified, then were confirmed by DNA sequencing. DNA sequencing confirmed the presence of CKM, CKMT1B and CKMT2 sequences inserted in frame into the multiple cloning site of the pcDNA4/TO vector. Two single base pair differences

(T440C, and T1193C) exist between the CKM insert sequence and the published CKM sequence (NCBI accession #BC007462). These synonymous substitutions do not alter the amino acid sequence of the protein. The CKMT1B insert sequence is identical to the published sequence (NCBI accession #NM020990). The CKMT2 insert sequence differs from the published sequence (NCBI accession #BC029140) by a single base pair (T280G) resulting in a serine to alanine amino acid substitution. The results from the initial PCR amplification and an enzymatic digest of the re-amplified maxiprep products are shown in Figure 3.6.

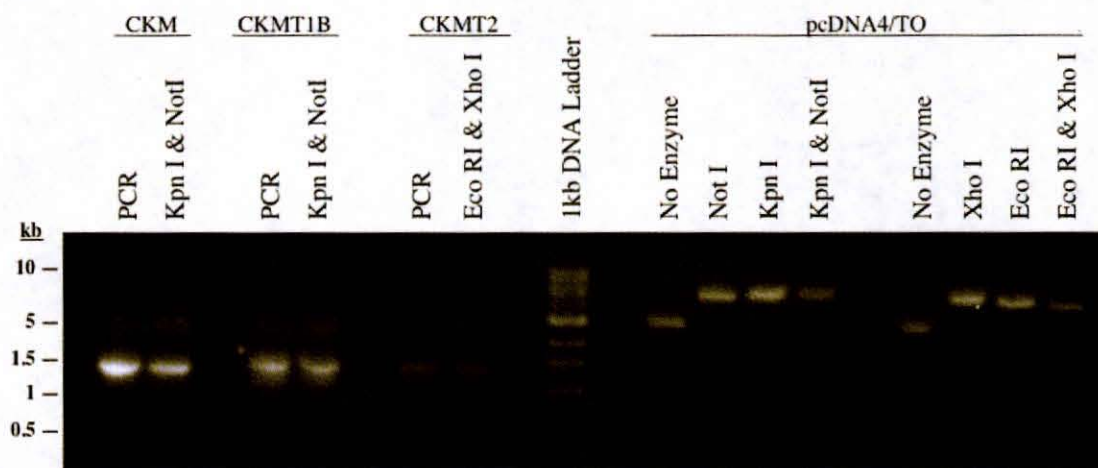


Figure 3.6. V5-CK insert and restriction enzyme digested CK-pcDNA4/TO constructs.

CKM (1146 bp) CKMT1B (1255 bp) and CKMT2 (1260 bp) DNA sequences with an C-terminal V5-epitope tag sequence were amplified by PCR and electrophoresed next to, restriction enzyme digested CK-pcDNA4/TO construct maxiprep products electrophoresed on a 1% agarose gel with ethidium bromide. Controls include; undigested pcDNA4/TO vector, single enzyme digested vector and double enzyme digested vector. Creatine kinase PCR products and digested inserts are observed at about 1.2 kb and pcDNA4/TO is observed at about 5 kb.

TRPA1 interacts with CKM, CKMT1B and CKMT2.

The interactions between non-brain specific creatine kinase isoforms (CKM, CKMT1B and CKMT2) and TRPA1 were confirmed in AFC cells. To achieve this, 0.5 - 2 μ g of the V5-CK pcDNA4/TO constructs (see materials and methods) were transiently lipid transfected into AFC cells induced to over-express FLAG-TRPA1. Proteins from the lysates of these cells were immunoprecipitated with the anti-FLAG antibody. Immuno-complexes were separated by SDS-PAGE and detected on a western blot with FLAG and V5 antibodies.

The FLAG antibody again detected FLAG-TRPA1 protein (predicted molecular weight 127 kDa) and another protein of higher molecular weight (>250 kDa) (Figures 3.7-3.9). The FLAG antibody heavy (50 kDa) and light (25 kDa) chain proteins were also present in all western blots, however the light chain is not shown in some figures. The V5 antibody detected co-immunoprecipitated V5-CK proteins (predicted molecular weights; CKM 43 kDa, CKMT1B 47 kDa and CKMT2 48 kDa). Similar to results in Figure 3.1, the relative amounts of V5-CK proteins detected on the western blots appear to correspond to the amount of the corresponding construct transformed into the cells. The V5 antibody also detected additional proteins, in Figures 3.8 and 3.9, of lower molecular weight than the non-brain V5-creatine kinase proteins.

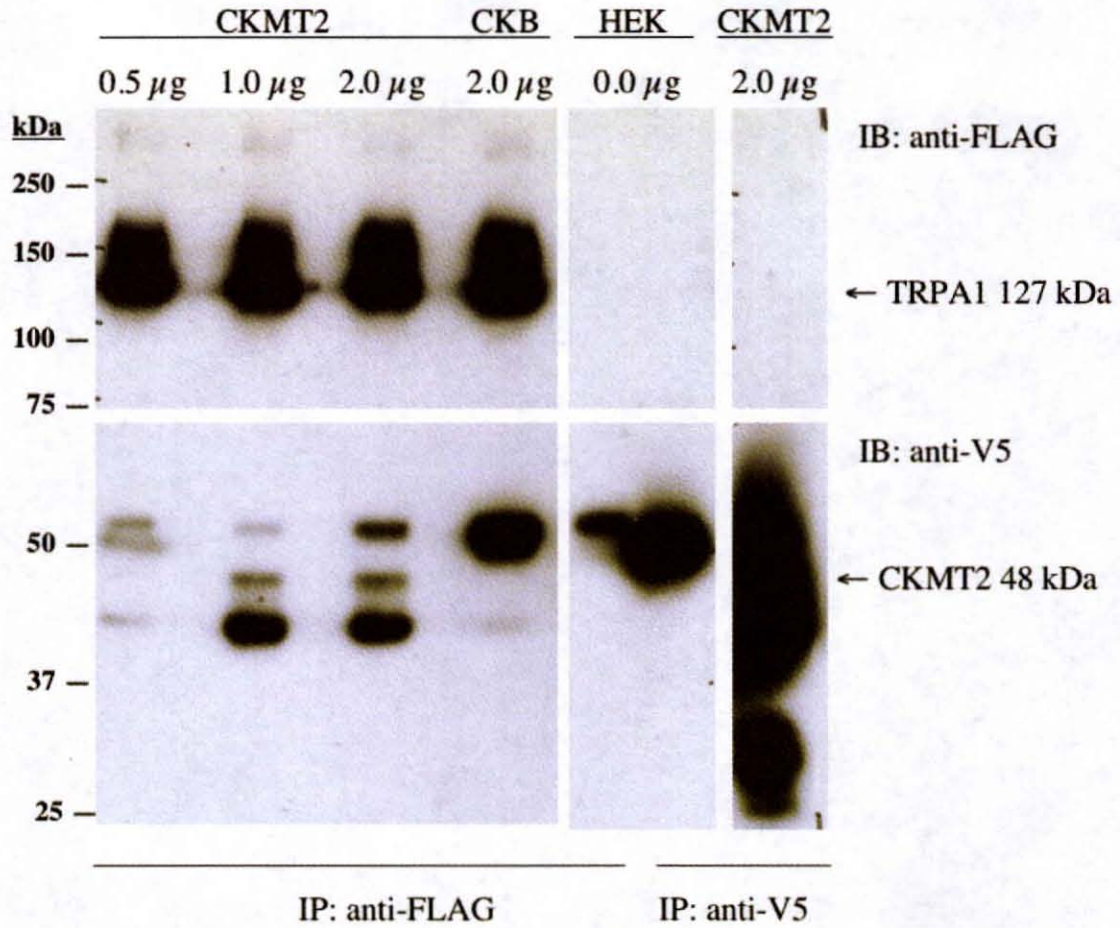


Figure 3.7. Western blot showing co-immunoprecipitation of V5-CKM by FLAG-TRPA1.

0.5 μ g, 1.0 μ g, or 2 μ g of the pcDNA 4/TO V5-tagged creatine kinase CKM construct was lipid transfected into HEK293Trex-TRPA1-FLAG cells. Cells were lysed and immunoprecipitated using 7.1 μ g/ml FLAG antibody. Immunocomplexes were resolved by SDS-10% PAGE and detected on western blots using antibodies against FLAG and V5. The predicted molecular weight for TRPA1 is 127 kDa and CKM is 43 kDa. Antibody heavy and light chain proteins are also observed at 50 kDa and 25 kDa.

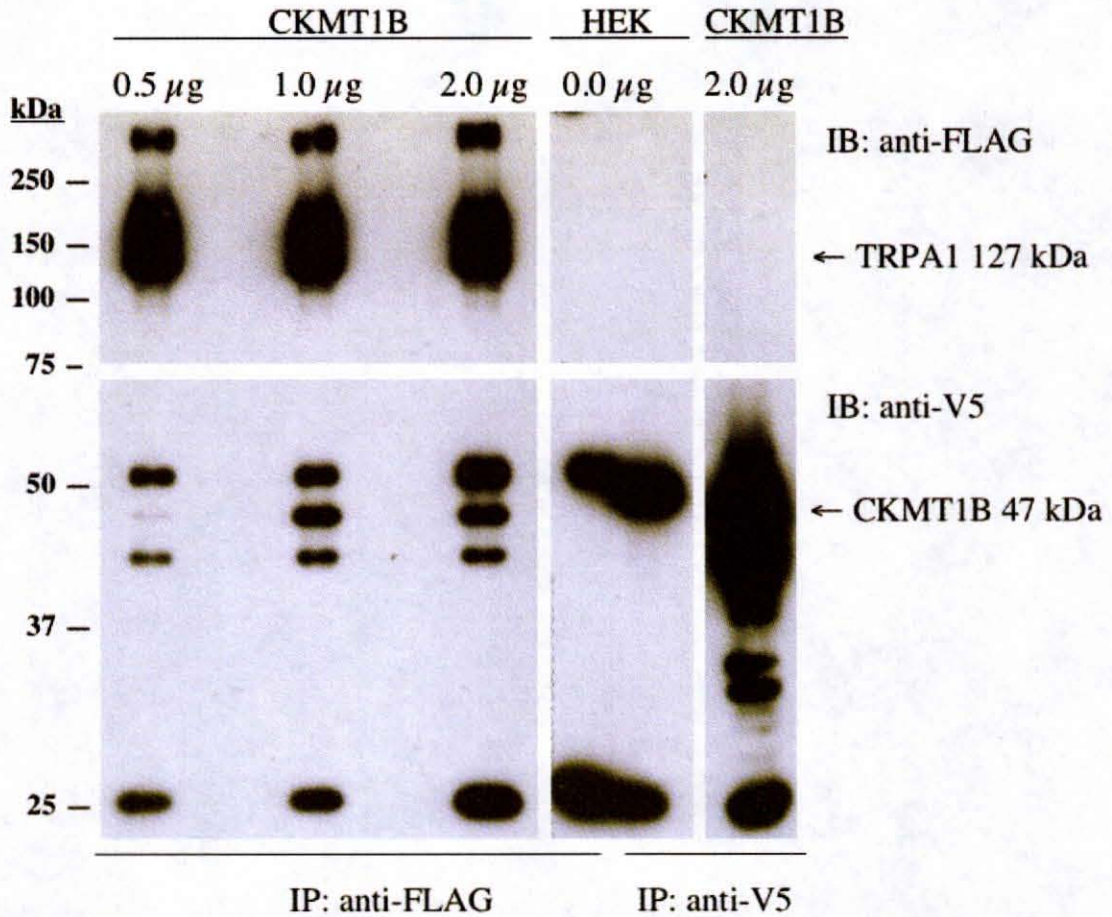


Figure 3.8. Western blot showing V5-CKMT1B co-immunoprecipitation by FLAG-TRPA1.

0.5 μ g, 1.0 μ g, or 2 μ g of the pcDNA 4/TO V5-tagged CKMT1B construct was lipid transfected into HEK293Trex-TRPA1-FLAG cells. Cells were lysed and immunoprecipitated using 7.1 μ g/ml FLAG antibody. Immunocomplexes were resolved by SDS-10% PAGE and detected on western blots using antibodies against FLAG and V5. The predicted molecular weight for TRPA1 is 127 kDa and CKMT1B 47 kDa. Antibody heavy and light chain proteins are also observed at 50 kDa and 25 kDa.

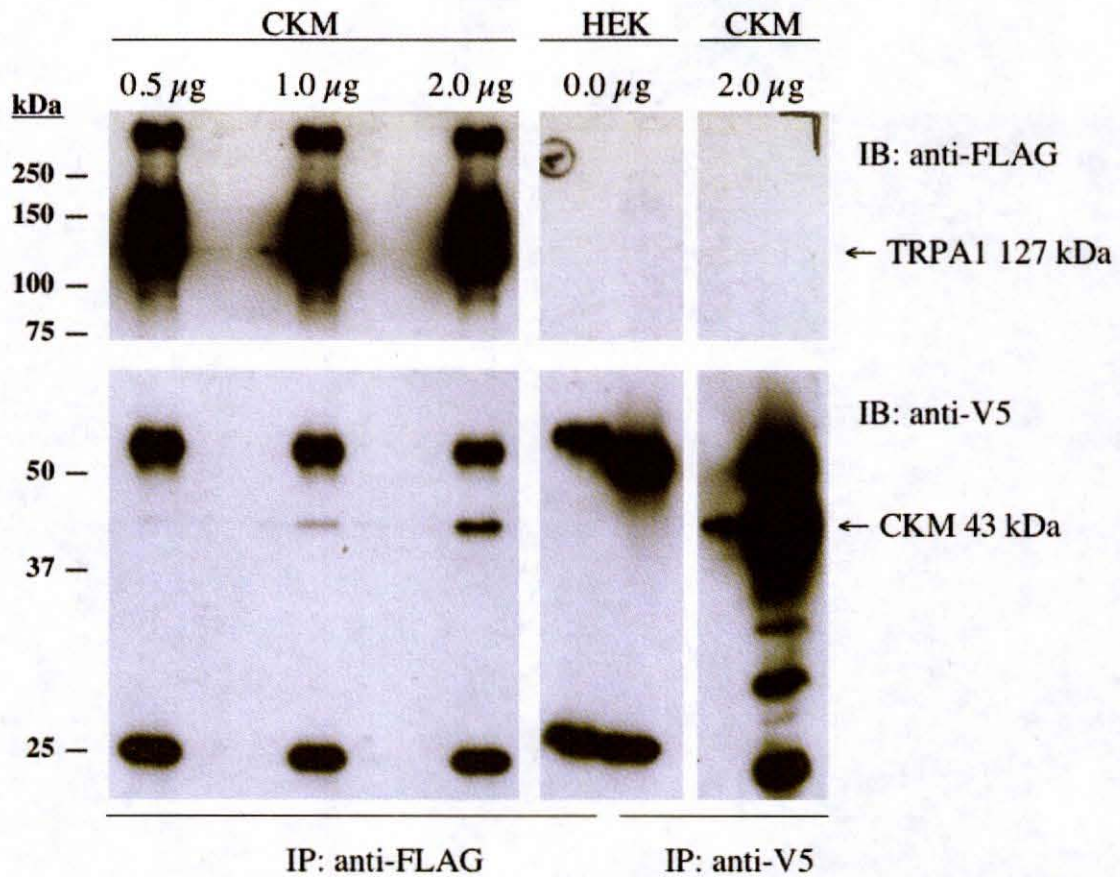


Figure 3.9. Western blot showing V5-CKMT2 co-immunoprecipitation by FLAG-TRPA1.

0.5 μ g, 1.0 μ g, or 2 μ g of the pcDNA 4/TO V5-tagged CKMT2 construct was lipid transfected into HEK293Trex-TRPA1-FLAG cells. Cells were lysed and immunoprecipitated using 7.1 μ g/ml FLAG antibody. Immunocomplexes were resolved by SDS-10% PAGE and detected on western blots using antibodies against FLAG and V5. The predicted molecular weight for TRPA1 is 127 kDa and CKMT2 is 48 kDa. Antibody heavy and light chain proteins are also observed at 50 kDa and 25 kDa.

3.3 Discussion

These results confirm that over-expressed FLAG-TRPA1 and V5-CK isoforms interact in total lysate from HEK cells. The identification of interactions between over-expressed proteins does not prove that the endogenous CK and TRPA1 proteins interact. Additionally, interactions that are observed between over-expressed proteins in cell lysate might not occur in intact cells because proteins could be separated by physical barriers due to localization in different subcellular regions.

Interactions between the endogenous proteins could be confirmed by co-immunoprecipitation experiments in HEK cells with antibodies against endogenous TRPA1 and various CK proteins. Immunostaining of whole cells to characterize localization patterns of the TRPA1 and CK proteins could also help to determine whether the proteins are likely to interact *in vivo*. Fluorescence Resonance Energy Transfer experiments could also be designed to characterize the interaction between fluorophore-tagged proteins *in vivo*. The sub-cellular localization of TRPA1 protein is explored in Chapter 4 providing another method for the identification of potential locations for physiological interactions.

These western blot results are insufficient to confirm a direct interaction between the over-expressed proteins, because the antibodies used for western blotting detected only the over-expressed FLAG and V5 tagged proteins. The observed interaction may require mediation by undetected additional factors that are present in the cell lysate. One potential example is that, the interaction of TRPA1 with only one isoform of creatine kinase could be sufficient to co-immunoprecipitate the other isoforms. The formation of

hetero-oligomers between endogenous and over-expressed creatine kinase isoforms forms could mediate interactions with additional isoforms. The presence of additional creatine kinase isoforms in the immunocomplexes could be detected with antibodies specific to the various isoforms. Blue Native PAGE (BN-PAGE) could also be used to identify non-reduced oligomers and immunocomplexes. Further methods of investigating the nature of these interactions through the production of His-tagged proteins are described in Chapter 5. Results from preliminary pull-down assays, using the His-tagged proteins to assess binding affinity between the TRPA1 cytoplasmic terminals and CKM are discussed in Appendix B.

The FLAG antibody consistently detected proteins at the predicted molecular weight of TRPA1 (127 kDa) and at higher molecular weight (>250 kDa). These proteins are recognized by both FLAG (c-terminal) and TRPA1 (c-terminal) antibodies (see chapter 4) thus likely contain TRPA1 protein. The higher MW band may indicate non-reduced protein oligomers or complexes, in which proteins are bound to one another or to other molecules in a manner that confers resistance to reducing agents. This band could also represent a form of TRPA1 protein that has been modified post-translation.

The V5 antibody detected multiple proteins of lower molecular weight than those predicted for the V5-creatine kinases (43–48 kDa). These proteins are likely partially digested segments of the creatine kinase monomer that consists of a stable C-terminal domain separated from a less stable N-terminal domain by an unfolded central region that is highly sensitive to digestion by proteases. (Webb et al., 1997) The V5 epitope tag was

incorporated at the C-terminal of the creatine kinase proteins, so detection of the proteins with the V5 antibody implies retention of the C-terminal domain.

The serine (S) to alanine (A) amino acid substitution found in the CKMT2 insert DNA sequence could change the structure of the associated CKMT2 protein and might have an effect on the activity or regulation of the protein. In this case, it is unlikely that the protein conformation would be altered because, alanine and serine are both small and occupy a similar volume (van der Waals volume A=67 and S=73). These amino acids both have neutral pH, however alanine is nonpolar with aliphatic R groups and serine is polar with uncharged R groups. The hydrogen of the serine hydroxyl group is easy to remove, which allows serine to act as a hydrogen donor in enzymes. Serine is important for the catalytic function of many enzymes thus the substitution of serine to alanine, which is non-reactive and rarely involved in protein function, might affect the function of CKMT2. Enzyme activity assays could be done to determine whether this substitution has an effect on the enzymatic activity of CKMT2.

The results of the co-immunoprecipitation experiments shown in this chapter accomplish the goal of validating the interaction between human TRPA1 protein and the four human creatine kinase protein isoforms in a human cell environment. Future research could validate the interaction between the endogenous proteins *in vivo* and further characterize the interaction.

CHAPTER 4: LOCALIZATION OF TRPA1 EXPRESSION

4.1 Introduction

TRPA1 has been studied extensively in neurons, where it functions as a channel in the plasma membrane. The results presented in Chapter 3 confirmed interactions between over-expressed TRPA1 protein and over-expressed creatine kinase protein isoforms, including those expressed endogenously in the mitochondria. These results combined with preliminary electron microscopy data suggest that TRPA1 might also be expressed and function in mitochondrial membranes. Human embryonic kidney (HEK) cells were immunostained with antibodies against TRPA1 and various subcellular marker dyes, however the results were inconclusive and are not shown. Results that are presented in this chapter identified TRPA1 protein in subcellular fractions of HEK cells containing proteins from mitochondria and other organelles.

TRPA1 functions as transducer of sensory stimuli in neurons, however, it is also expressed in non-neuronal cell and tissue types where its function is unknown. The identification of TRPA1 in subcellular fractions of non-neuronal cells suggests that it might function in the intracellular membranes of these tissues. Western blot results presented in this chapter confirmed the expression of TRPA1 protein in multiple non-neuronal tissues. Western results also showed that levels of TRPA1 protein expression in these tissues did not correspond with expression levels of the mitochondrial protein Pyruvate dehydrogenase-e1 α (PDHe1 α), which demonstrated that TRPA1 protein expression was not higher in human tissues enriched in mitochondria.

4.2 Results

Sub-cellular Expression of TRPA1

Total lysate from non-induced HEK293TRex cells expressing was separated into fractions by various forms and speeds of centrifugation. Protein fractions, containing equal amounts of total protein were separated by SDS-PAGE and analyzed by western blot using an antibody raised against the c-terminal tail of TRPA1. Antibodies against well-characterized intracellular markers including; cyclin B1 (nuclear), PMP-70 (peroxisomal), PDHe1 α (mitochondrial), and VDAC (mitochondrial), were used to help verify the composition of the subcellular fractions. The Grb2 antibody was also used to demonstrate the presence of protein in each lane because Grb2 is widely distributed throughout the cell. Subcellular fractions for the blot in Figure 4.1 were separated using protocol 1 (see Materials and Methods). The fractions for the blot in Figure 4.2 were separated using protocol 2 (see Materials and Methods), where the mitochondrial, endoplasmic reticulum (ER), and lysosomal/peroxisomal (L/P) fractions were further separated by ultracentrifugation over sucrose gradients.

The western blot results shown in Figures 4.1 and 4.2. indicated that overall the expression of TRPA1 monomer (127kD) was at the highest concentration in fractions containing the ER and plasma membrane. Nuclear proteins may be present in the ER fractions as evidenced by strong cyclin B1 signal, however the nuclear fractions also contained strong cyclin B1 signal and contained much weaker TRPA1 bands. The ER

fractions contained little to no signal with antibodies against VDAC, PDHe1 α and PMP-70 indicating low levels of peroxisomal and mitochondrial proteins.

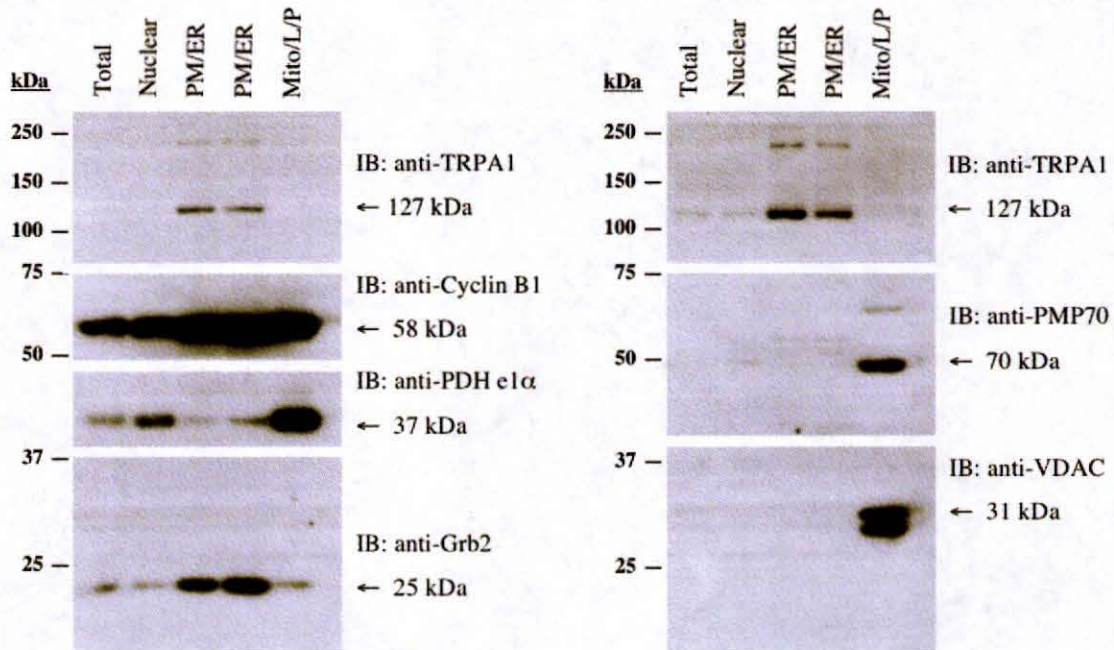


Figure 4.1. Enriched TRPA1 protein expression in subcellular PM/ER fractions.

HEK293Trex cells were mechanically lysed then separated by differential centrifugation into fractions containing total, nuclear, plasma membrane (PM)/endoplasmic reticulum (ER) and mitochondrial/lysosomal (L)/peroxisomal (P) proteins. (Protocol 1 in Materials and Methods). Protein fractions were separated by SDS-10% PAGE and visualized by western blot. The blot was cut into sections, which were incubated with antibodies against TRPA1 (127 kDa) and various subcellular components; cyclin B1 (58 kDa, nuclear), PMP-70 (70 kDa, peroxisomal), PDHe1 α (37 kDa, mitochondrial), and VDAC (31 kDa, mitochondrial). The Grb2 (25 kDa) antibody was used to demonstrate the presence of proteins in each lane.

Results in Figure 4.2 show that the high molecular weight TRPA1 band was enriched in the mitochondrial fraction that also contains high levels of the mitochondrial proteins PDHe1 α and VDAC. Overall, the expression of TRPA1 (127kD) was found to be at its highest concentration in the fraction containing the ER and plasma membrane, which may be contaminated with nuclear proteins as evidenced by a strong band in the portion of the blot probed with the cyclin B1 antibody.

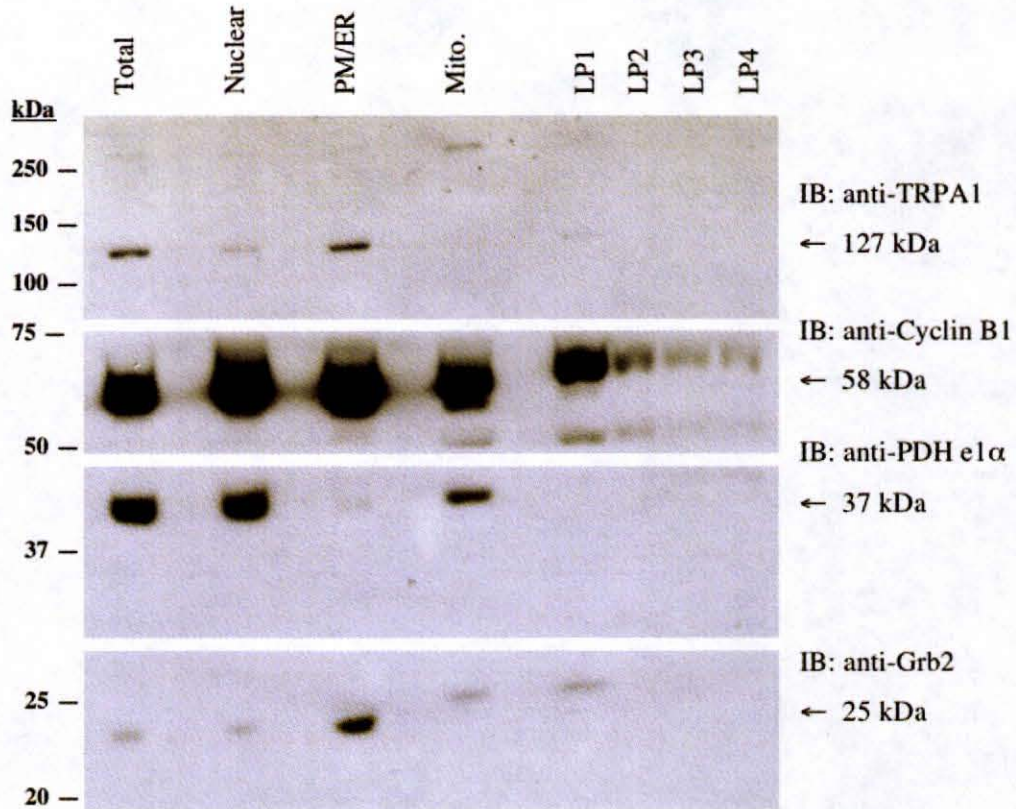


Figure 4.2. High MW TRPA1 protein expression is enriched in mitochondrial fractions.

HEK293TRex cells were mechanically lysed then separated by differential centrifugation into fractions containing total, nuclear, plasma membrane (PM)/endoplasmic reticulum (ER) and mitochondrial/lysosomal (L)/peroxisomal (P) protein fractions. Following Protocol 2 (Materials and Methods), these fractions were further separated by ultracentrifugation over sucrose gradients to isolate ER, L/P, and more pure mitochondrial proteins. Samples were separated by SDS-10% PAGE and visualized by western blot with antibodies against TRPA1 (127 kDa), cyclin B1 (58 kDa, nuclear) and PDHe1 α (37 kDa, mitochondrial). The Grb2 (25 kDa) antibody was used to demonstrate the presence of proteins in each lane.

Expression of TRPA1 in Human Tissues

Commercially available human tissue lysates (Biochain) were boiled in 1X final volume of reducing sample buffer and analyzed by SDS-PAGE. Proteins were detected on a western blot with antibodies against TRPA1 and PDH ϵ 1 α , a well-characterized mitochondrial marker, to determine the level of TRPA1 expression in various tissues and compare this to the level of mitochondria enrichment in these tissues. Grb2 antibody was used again to control for the presence of proteins in all samples. The results demonstrated expression of TRPA1 protein predominantly in human colon, where multiple protein bands were detected. TRPA1 protein expression was also detected in uterus, stomach, ovary and skin tissue. Enriched expression of the mitochondrial protein PDH ϵ 1 α was not detected in these tissues, however it was detected in tissues generally known to be enriched in mitochondria such as the brain, heart and skeletal muscle.

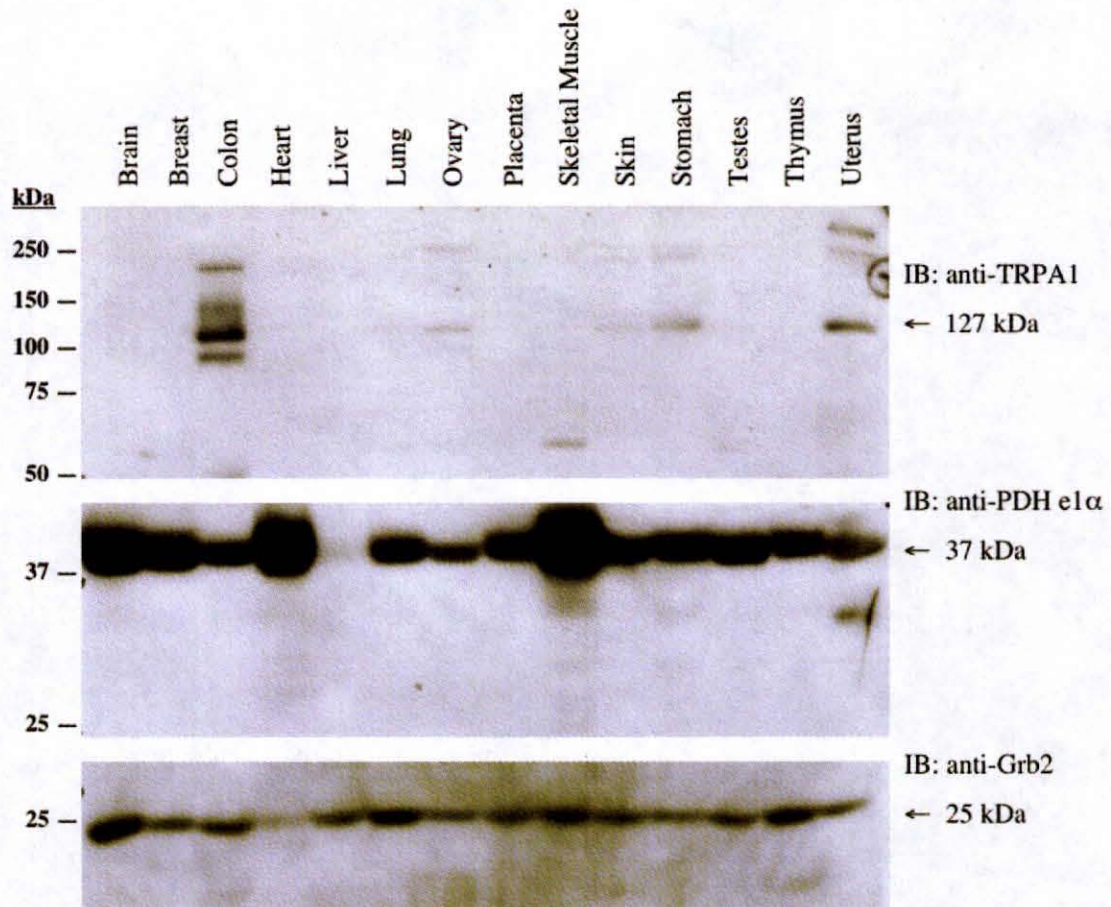


Figure 4.3. TRPA1 protein expression in human tissue lysates.

Western blot analysis demonstrates expression of TRPA1 predominantly in human colon, uterus, stomach, ovary and skin tissues. Total protein lysates from human tissues (50 mg, Biochain, CA) were boiled in reducing sample buffer, resolved by SDS-10% PAGE, and detected by western blot with antibodies against TRPA1 (127 kDa) and PDH e1 α (37 kDa). The bottom panel shows a portion of the blot that was re-probed with an antibody against Grb2 (25 kDa) to confirm the presence of protein in all lanes.

4.3 Discussion

The subcellular fractionation results demonstrate enriched TRPA1 protein levels in the intracellular fraction that includes the plasma membrane and ER. This suggests that TRPA1 channels may function in regulating calcium influx across the plasma membrane of non-neuronal cells, just as they do in neuronal cells. Results from the immunostaining of HEK cells with antibodies against TRPA1 and various subcellular markers were inconclusive. However, additional immunostaining could be done to further characterize the expression pattern of TRPA1 in the membranes and compartments of intact cells. Functional localization of TRPA1 protein at the plasma membrane of non-neuronal cells could be demonstrated using patch clamp experiments to characterize TRPA1 channel activity at the plasma membrane.

Based on the fractionation results, TRPA1 protein may also be expressed in the ER of non-neuronal cells. It is generally regarded that TRP channel proteins are synthesized in the ER, where they can form oligomers (briefly) prior to being transported as tetramers to the destined membranes. The detection of newly synthesized, thus not functionally active, TRPA1 proteins may explain the detection of TRPA1 in fractions containing ER. Pulse chase experiments could be used to track the synthesis and trafficking of TRPA1 proteins and determine the length of time they spend in various intracellular locations.

The TRPA1 antibody also detected mitochondrial enrichment of protein with a molecular weight protein of 250 kDa (larger than the predicted 127 kDa). This protein was also detected with the FLAG antibody in the results presented in Chapter 3, where it

is discussed in more detail. Enrichment of this protein band in mitochondrial fractions suggests that a modified or oligomeric form of TRPA1 may be present and function within the mitochondria. The identification of TRPA1 protein in the subcellular fraction containing mitochondrial suggests that the observed interaction between TRPA1 and the mitochondrial creatine kinase isoforms could occur directly in the mitochondria. Perhaps interaction with creatine kinase results in non-reducible modifications of TRPA1 proteins or stabilization of associated complexes (possibly oligomers) that account for the higher molecular weight proteins that were detected by the TRPA1 antibody.

TRP channels, including TRPM8 and TRPV1 are expressed in the intracellular membranes where they regulate the release of calcium from intracellular stores like the ER and golgi. (Mahieu et al., 2007; Turner et al., 2003) Given its potential expression in intracellular protein fractions, TRPA1 may also function in the regulation of calcium release from intracellular stores. Investigation of the role of TRPA1 in regulating the release of calcium from intracellular stores has been initiated utilizing Fura2-AM dye to identify changes in intracellular calcium levels. Preliminary experiments and the results obtained from them are discussed in Appendix A.

The tissue blot reveals enrichment of TRPA1 protein in human colon, uterus, stomach, ovary and skin tissues. In addition to the 127 kD TRPA1 protein, the higher molecular weight protein, discussed in Chapter 3, was detected in all of these tissues. The TRPA1 antibody also detected an additional ~90 kDa protein band in the colon. This band may represent a modified or degraded form of TRPA1 protein. All of the tissues shown to express TRPA1 are contractile and contain smooth muscle fibers. These results

agree with previously demonstrated enrichment in contractile tissues including the small intestine (western and northern blots) and colon (northern blot). (Stokes et al., 2006)

TRRPA1 expression is not apparent in the brain and heart tissues of the multi-tissue western blot presented in this chapter. This contradicts the results of previous research where TRPA1 enrichment was demonstrated in brain and heart tissues (western blot). (Stokes et al., 2006) TRPA1 is known to function in peripheral neuro-sensory cells, including dorsal root ganglion cells, however it is not necessarily enriched in brain tissue. Differences in the amounts of protein loaded on the western blots or in the preparation of tissue lysates could account for differences in the levels of TRPA1 protein detected in the various tissues. Based on previous and current results it is unclear whether TRPA1 is expressed in tissues enriched in mitochondria. The tissue distribution of TRPA1 expression could be confirmed by additional immunostaining of various tissues and cells.

It is important to note that Grb2 is a useful tool to demonstrate the presence of protein in individual samples, however, it is not a reliable indicator of the total amount of protein loaded in each well. Despite the wide distribution of Grb2 throughout the cell, the level of its expression may vary in different subcellular compartments.

The results of the cellular fractionation experiments confirm that the TRPA1 antibody detects enrichment of a high molecular weight protein in subcellular human cell fractions that contain mitochondrial proteins. The results are not sufficient to determine whether TRPA1 is actually expressed in the mitochondrial membranes of intact cells.

Future research could further characterize the TRPA1 protein expression pattern various cell types and cellular membranes.

CHAPTER 5: DEVELOPMENT OF TOOLS FOR FURTHER STUDY OF THE INTERACTION BETWEEN TRPA1 AND CREATINE KINASE

5.1 Introduction

Protein-protein interactions can occur directly through binding of one protein to another through intrinsic protein binding domains. However, many protein-protein interactions require post-translational protein modifications or may require mediation by small molecules or other proteins present in the cell. The interaction between TRPA1 and CKB was initially identified by the SRS system in yeast, where post-translational protein modifications associated with mammalian proteins would not likely occur. In addition, yeast do not contain proteins and small molecules typical of the mammalian cell environment that could mediate protein interactions in human cells, like those described in Chapter three. Therefore, identification of the interaction between in the TRPA1 cytoplasmic tail and rat CKB proteins by the Sos-recruitment system (SRS) in yeast suggests a direct interaction between the two proteins.

Results presented in chapter three confirmed that the interaction between TRPA1 and all four of the human creatine kinase isoforms occurred in HEK293TRex cells. The SRS assay demonstrated an intracellular interaction between the human TRPA1 cytoplasmic tail and rat CKB. Results presented in this chapter demonstrate the generation of purified histidine-tagged cytoplasmic, carboxyl and amino terminal fragments of the TRPA1 protein, in addition to full-length muscle-type creatine kinase proteins. The chapter also describes methods by which these proteins could be used to

determine whether the interaction between one of the creatine kinase isoforms, CKM and TRPA1 is direct, and if the interaction occurs through either of the cytoplasmic tails of TRPA1.

5.2 Results

Sub-cloning and Expression of His-tagged Constructs

PCR primers for TRPA1 fragments were designed to target the cytosolic amino (amino acids #1-725) and carboxyl (amino acids # 961-1119) terminals of TRPA1. Terminal sequences were determined based on transmembrane domain predictions from a Kyte/Doolittle hydrophobicity plot (MacVector, Accelrys) shown in Figure 5.1 and the SOSUI system (http://bp.nuap.nagoya-u.ac.jp/sosui/sosui_submit.html). Target cDNA sequences for TRPA1 terminals and CKM were amplified by PCR and subsequently subcloned into the pTrcHisB vector. The pTrcHisB vector (Figure 2.1) is a pBR322 derived expression vector, designed for production of recombinant protein in *E. coli*. This vector confers a six Histidine tag sequence that allows the purification and detection of His-tagged protein. The vector also contains an enterokinase cleavage site that allows removal of the His-fusion tag. PCR primer sequences are presented in Table 2.2 followed by PCR reaction conditions in the materials and methods section.

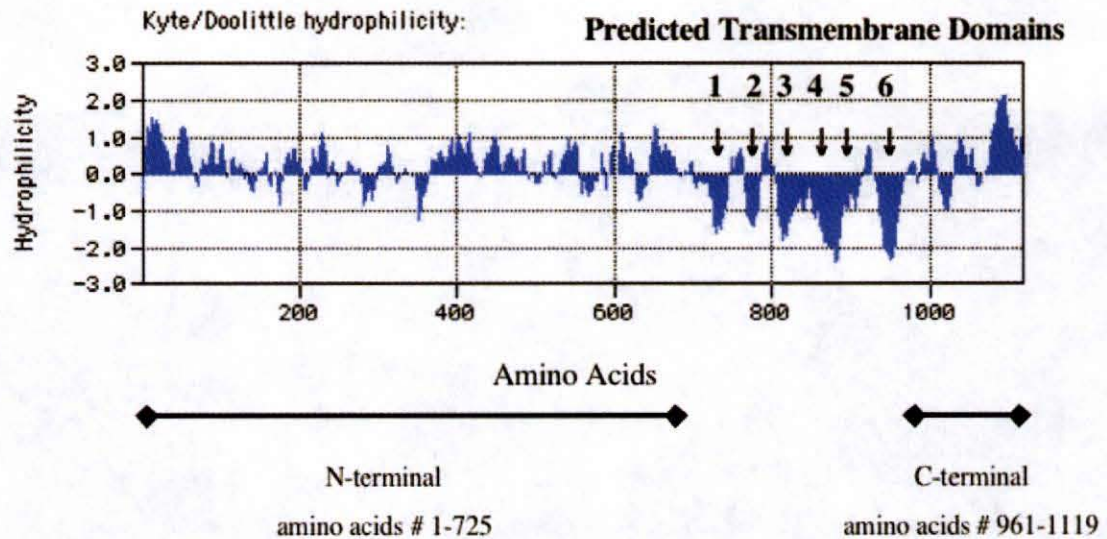


Figure 5.1. Kyte/Doolittle hydrophathy plot prediction of TRPA1 transmembrane domains.

Kyte-Doolittle hydrophathy plot (MacVector, Accelrys) prediction of potential transmembrane and surface regions within the structure of a protein. Amino acid hydrophobicity scores are based on a combination of the side chains' water-vapor transfer free energies and preference for interior or exterior environments. The y-axis represents the hydrophilicity scores and the x-axis represents the amino acid sequence number. Regions with values below zero are hydrophobic in character thus are likely candidates for transmembrane domains that are not exposed on the protein's surface. (Kyte and Doolittle, 1982)

All three constructs were subcloned into the pTrcHisB vector using Kpn I and Xho I restriction enzymes. An overview of the subcloning strategy is shown in Figure 5.2.

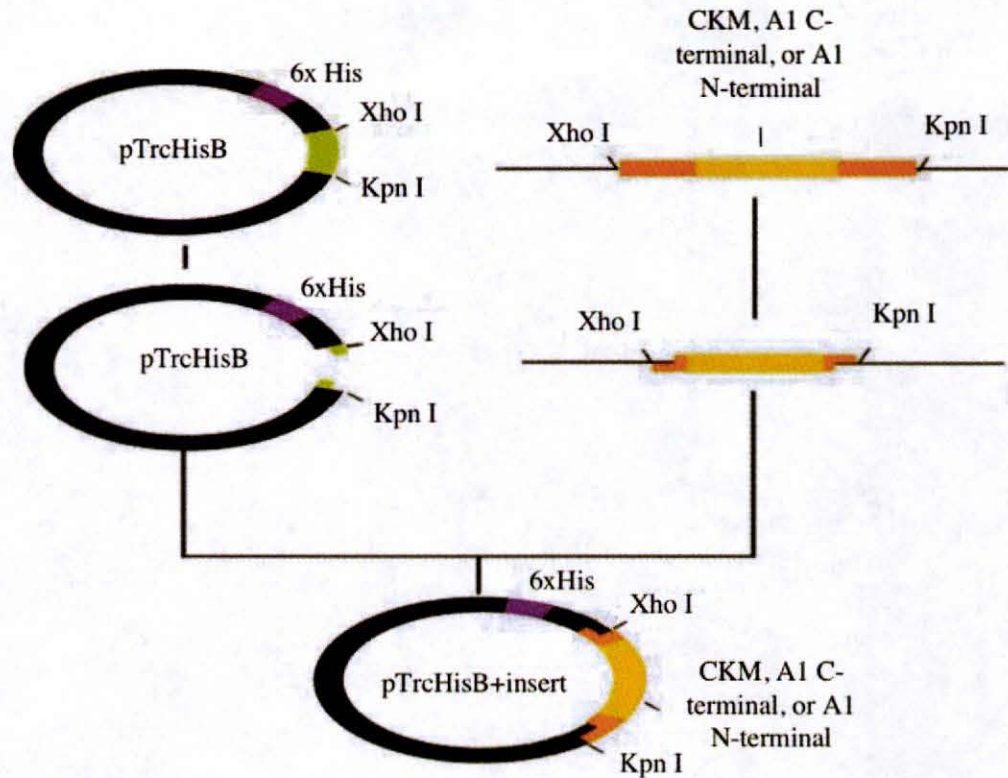


Figure 5.2. pTrcHisB vector subcloning schematic.

Insert DNA is amplified by PCR with primers that confer XhoI and KpnI restriction enzyme cut sites. The PCR products and pTrcHisB vector are digested with both enzymes, then ligated together to form constructs which are transformed into, expressed in and isolated from competent *E. coli*. Final construct composition is confirmed by DNA sequencing.

The results from an enzymatic digest of the subcloning products are shown in figure 5.3. All samples digested with both restriction enzymes contain the pTrcHisB vector (~5 kb) and one of the following inserts: C-terminal (462 bp), N-terminal (2100 bp) and CKM (1146 bp). The C-terminal insert (highlighted in the red square) is faint in this exposure, which was chosen to maximize the viewing of the majority of the bands in the gel. The C-terminal insert is evident in the cutout of the highlighted section of the blot

(shown to the right of the larger blot) where the contrast has been increased. This gel indicates the presence of a C-terminal insert of less than 0.5 kb, however cannot be used to accurately estimate the size of this insert, because it is outside the range of the 1 kb DNA ladder used.

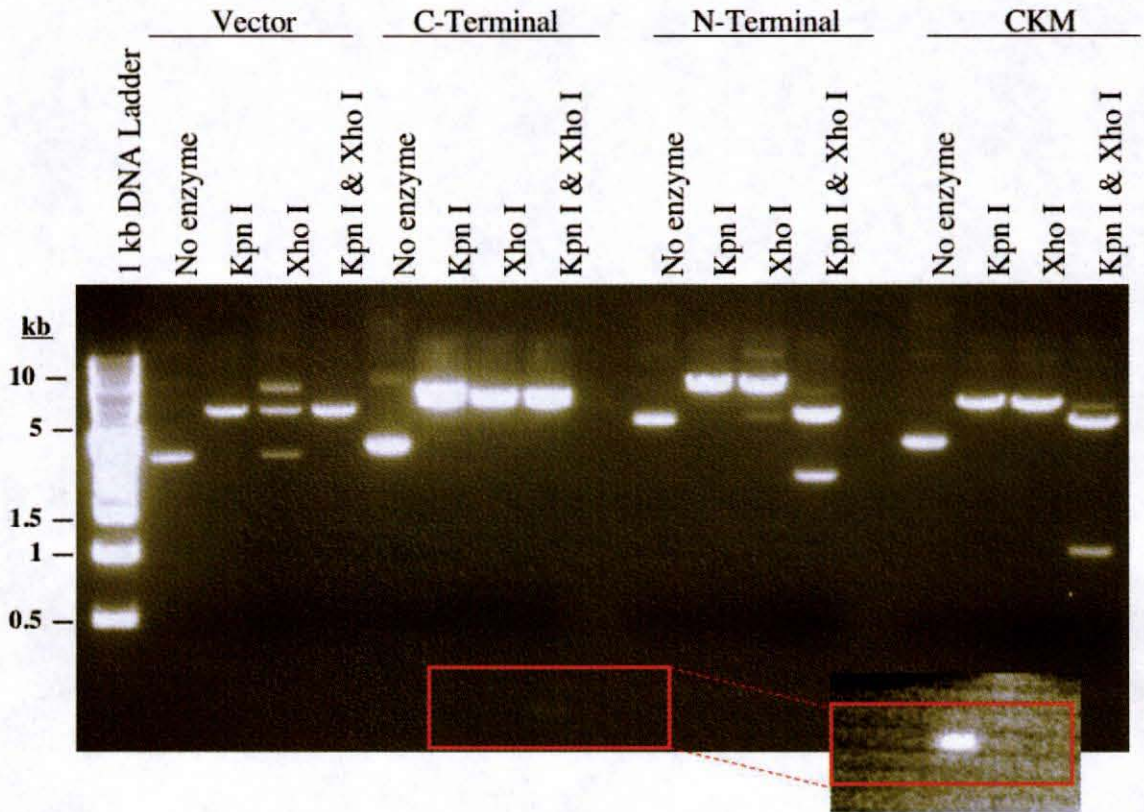


Figure 5.3. Enzymatic digest of CKM, TRPA1-N and TRPA1-C pTrcHisB constructs.

TRPA1 C-terminal (462 bp) and N-terminal (2100 bp) as well as CKM (1146 bp) DNA inserts were amplified by PCR, digested by KpnI and NotI restriction enzymes, then subcloned into the pTrcHisB vector. Restriction enzyme digested constructs were electrophoresed on a 1% agarose gel with ethidium bromide. The inset shows a section of large blot highlighted in red with increased contrast.

DNA sequencing confirmed that CKM, TRPA1 C-terminal and TRPA1 N-terminal sequences were inserted in frame into the multiple cloning site of the pTrcHisB vector. These constructs were also visualized on an agarose gel after enzymatic digestion. The TRPA1 template DNA from our lab contains a single base pair substitution (T375C) from the published sequence on NCBI. This synonymous substitution does not change the occurrence of asparagine at this position in the protein sequence. There are no additional base pair differences between the TRPA1 terminal insert sequences and the published sequence for TRPA1. Single base pair differences are present in the CKM insert sequence (C380T, T680C, and T1120C), however none of these synonymous substitutions alters the amino acid sequence of the protein.

Expression and Purification of His-tagged Proteins

BL21 competent *E. coli* was selected as a bacterial expression system to yield high concentrations of soluble protein, without the presence of degrading proteases. Protein expression, in this system, is controlled by the *lac* operator, which has been engineered into the pTrcHisB vector, permitting binding of the Lac repressor to repress transcription. Protein expression is induced by the addition of IPTG. IPTG halts transcriptional repression when it is added to *E. coli* that have been grown to mid-log phase ($OD_{600}=0.6-0.8$). His-tagged protein expression in the presence and absence of IPTG induction was confirmed using Coomassie Blue staining, shown in Figure 5.4. The presence of increased proteins in the culture with IPTG may be due to the addition of IPTG or may be

the result of increased protein production over time, since the culture at 2.5 hours with IPTG has an OD₆₀₀ of 0.8 compared to the culture prior to IPTG addition at 2 hours that has an OD₆₀₀ of 0.6.

The Immobilized Metal Affinity Chromatography (IMAC) technique was employed to purify the His-tagged proteins under native conditions. Specifically, His-tag affinity-binding column chromatography kit from Novagen was used on total soluble proteins extracted from BL21 *E. coli* cells. This kit employs the two different binding affinities between the series of six Histidine residues to metal (Ni²⁺) beads and imidazole. The kit requires that the total soluble proteins be run through a column filled with Ni²⁺ charged beads, to which the His-tagged proteins will bind. The final elution solution contains imidazole, which binds histidine with higher affinity than the Ni²⁺ beads. Thus, the His-tagged proteins are eluted in the imidazole buffer. The eluted protein samples are dialyzed to remove imidazole and reduce salt concentrations, preparing them for coupling to affinity supports and use in affinity assays.

Coomassie Blue staining in Figure 5.4 demonstrates the expression and purification of a 43 kDa protein, which is the approximate predicted size of CKM. Note that only one band remains after the resin has been washed and the band intensity is greatly reduced after the elution step. Contaminating proteins were washed away or are present at undetectable concentrations.

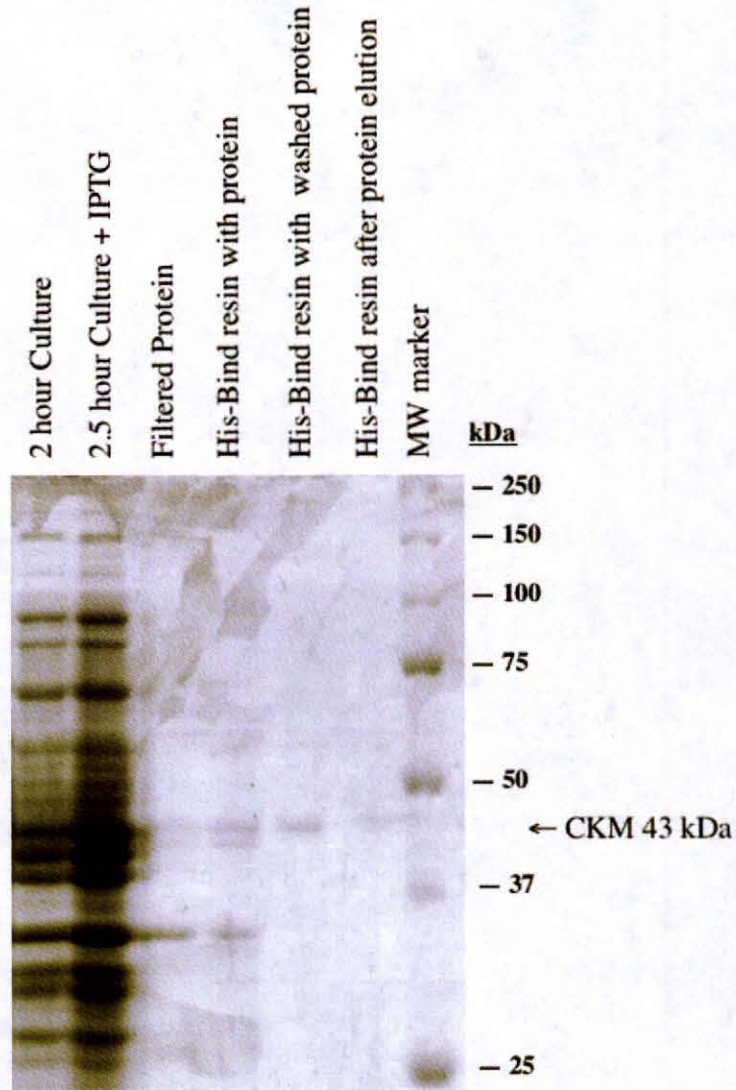


Figure 5.4. CKM protein expression and purification Coomassie blue stained gel.

BL-21 competent cells were transformed with the CKM-pTrcHisB construct. Protein expression was induced by addition of IPTG. Total soluble proteins were extracted from BL21 cells and purified by Ni²⁺ affinity chromatography with the His-bind kit. Protein samples were separated by SDS-10%PAGE and stained with Coomassie blue. Samples include total lysates from cultures prior to and after IPTG induction, filtered total proteins, samples of His-bind resin bound to filtered protein, after washing to remove non-specific binding, and after final elution of the His-tagged proteins. The predicted molecular weight for CKM is 43 kDa.

Western blot results in Figures 5.5-5.7 demonstrate the expression and purification of the His-tagged proteins. The His-tag antibody identified the CKM protein (predicted size 43 kDa) in most samples from the His-CKM protein purification (Figure 5.5). Lysates from HEK cells and HEK cells transiently transformed and induced to express the V5-CKM construct, contain a protein of similar size that was detected with a CKM antibody. The C-terminal TRPA1 protein (18 kDa, predicted using MacVector) was detected in samples from the corresponding protein purification (Figure 5.6), as was the N-terminal TRPA1 protein (79 kDa, predicted using MacVector) (Figure 5.7). Proteins of lower molecular weight are present in some of the elutions from the N-terminal protein purification.

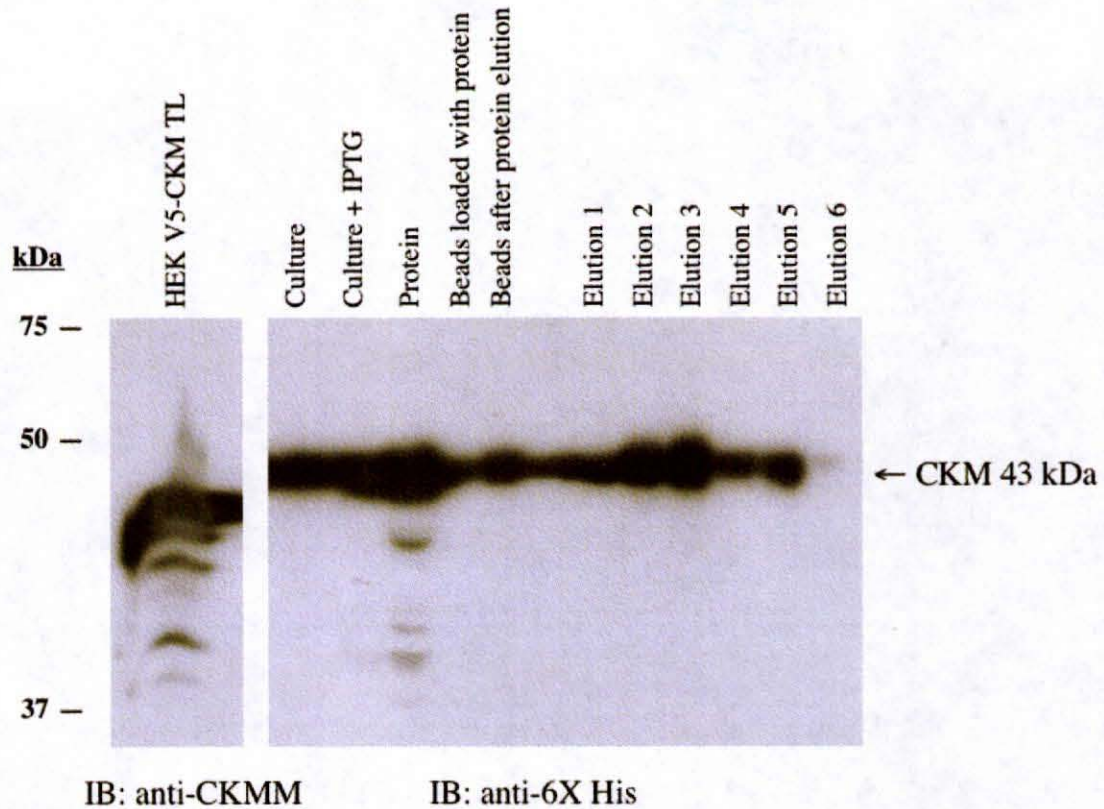


Figure 5.5. CKM protein expression and isolation western blot.

BL-21 competent cells were transformed with the CKM-pTrcHisB construct. Protein expression was induced by addition of IPTG. Total soluble proteins were extracted from BL21 cells and purified by Ni²⁺ affinity chromatography with the His-bind kit. Protein samples were separated by SDS-10%PAGE and western blotted with the 6X His-tag antibody. Protein samples include; total lysate from the IPTG induced BL-21 culture, filtered total protein, His-bind resin loaded with protein, His-bind resin following protein elution and eluted proteins. Left panel contains the total lysate of HEK cells transformed with 2 μ g CKM-pTrcHisB construct western blotted with the CKMM antibody as a positive control for the presence of CKM protein. The predicted molecular weight for CKM is 43 kDa.

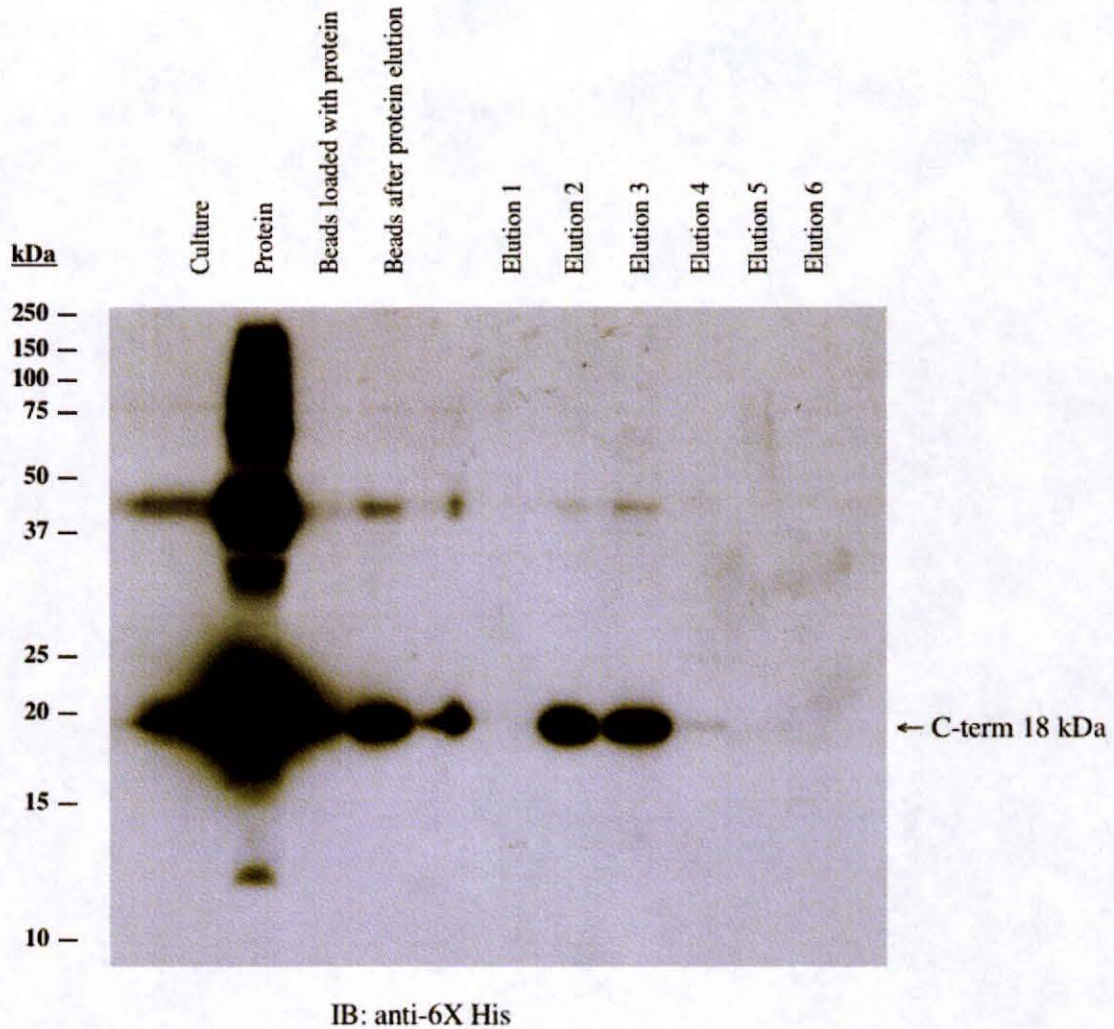
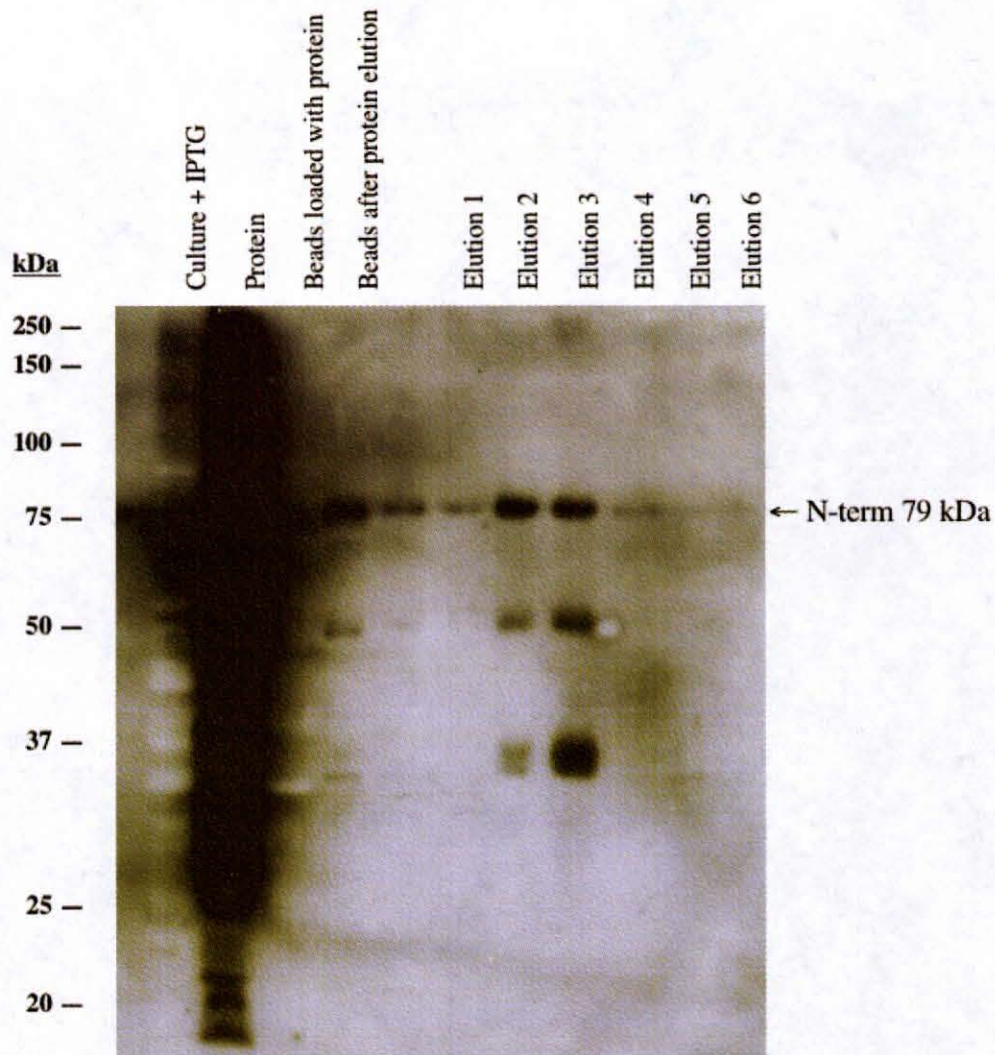


Figure 5.6. TRPA1 C-terminal protein expression and isolation western blot

BL-21 competent cells were transformed with the CKM-pTrcHisB construct. Protein expression was induced by addition of IPTG. Total soluble proteins were extracted from BL21 cells and purified by Ni²⁺ affinity chromatography with the His-bind kit. Protein samples were separated by SDS-10%PAGE and western blotted with the 6X His-tag antibody. Protein samples include; total lysate from the IPTG induced BL-21 culture, filtered total protein, His-bind resin loaded with protein, His-bind resin following protein elution and eluted proteins. The predicted molecular weight for the His-C-terminal TRPA1 protein 18 kDa.



IB: anti-6X His

Figure 5.7. TRPA1 N-terminal protein expression and isolation western blot

BL-21 competent cells were transformed with the CKM-pTrcHisB construct. Protein expression was induced by addition of IPTG. Total soluble proteins were extracted from BL21 cells and purified by Ni²⁺ affinity chromatography with the His-bind kit. Protein samples were separated by SDS-10%PAGE and western blotted with the 6X His-tag antibody. Protein samples include; total lysate from the IPTG induced BL-21 culture, filtered total protein, His-bind resin loaded with protein, His-bind resin following protein elution and eluted proteins. The predicted molecular weight for the His-N-terminal protein is 79 kDa.

5.3 Discussion

The results clearly demonstrate that histidine-tagged creatine kinase and TRPA1 carboxyl and amino terminal peptides were generated. Over-expressed V5-tagged CKM proteins were detected in total lysate from transfected HEK cells at approximately five kDa lower than the His-CKM protein (Figure 5.5). Changes in the weight or conformation of the protein resulting from the addition of the N-term fusion peptide (3kD) and spacer amino acids could account for this shift. This shift could also be the result of a post-translational modification that differs when the His-tagged protein is produced in either *E.coli* or mammalian (HEK) cells.

Degraded protein products are frequently generated in *E. coli* expression systems during over-expression due to various stresses to the bacteria, including over induction and a long culture period. The BL21 strain that was used has been engineered as protease deficient to minimize protein degradation. Proteins of lower molecular weight (than the 79 kDa N-terminal) were detected in TRPA1 N-terminal westerns. These could be degraded N-terminal proteins or proteins that were modified differently when expressed in *E. coli* as opposed to mammalian cells. These could also be other proteins that contain His-tags or bound non-specifically to the His-bind column. The composition of these bands has not been examined.

The future production of His-tagged CKM and TRPA1 carboxyl and amino terminal proteins will be facilitated by the protocols described in this chapter. In addition, ample amounts of purified His-tagged proteins have been produced for use in

future studies. These tools have been used in preliminary affinity binding assays to investigate the nature of the interaction between these proteins. The results of these assays as well as difficulties encountered with the assays are discussed in Appendix B. Additional binding assays could determine whether the interaction between TRPA1 and muscle-type creatine kinase is direct. Additional subcloning and mutagenesis strategies could also be used to produce shorter protein fragments and mutated proteins to determine the exact domains involved in the interaction.

CHAPTER 6: SUMMARY DISCUSSION

The activation and subsequent opening of TRPA1 channels in the plasma membrane of neurons, results in increased cytosolic calcium levels that contribute to the initiation and propagation action potentials. This mechanism of signal transduction enables neurons to integrate information from complex stimuli and respond to changes in the physical environment. (Julius and Basbaum, 2001; Peterlin et al., 2007) The results presented in this thesis confirm the presence of TRPA1 protein in non-neuronal cells and identifies TRPA1 protein in sub-cellular fractions containing mitochondrial proteins. These findings suggest that, in addition to its function in the plasma of neurons TRPA1 may play a novel physiological role in the intracellular membranes of non-neuronal cells. The results also identify interactions between over-expressed human TRPA1 and creatine kinase proteins. This suggests that creatine kinase may regulate TRPA1 channel activity. Figure 6.1 demonstrates how these findings might fit into a basic schematic of the mechanisms and results of TRPA1 activation.

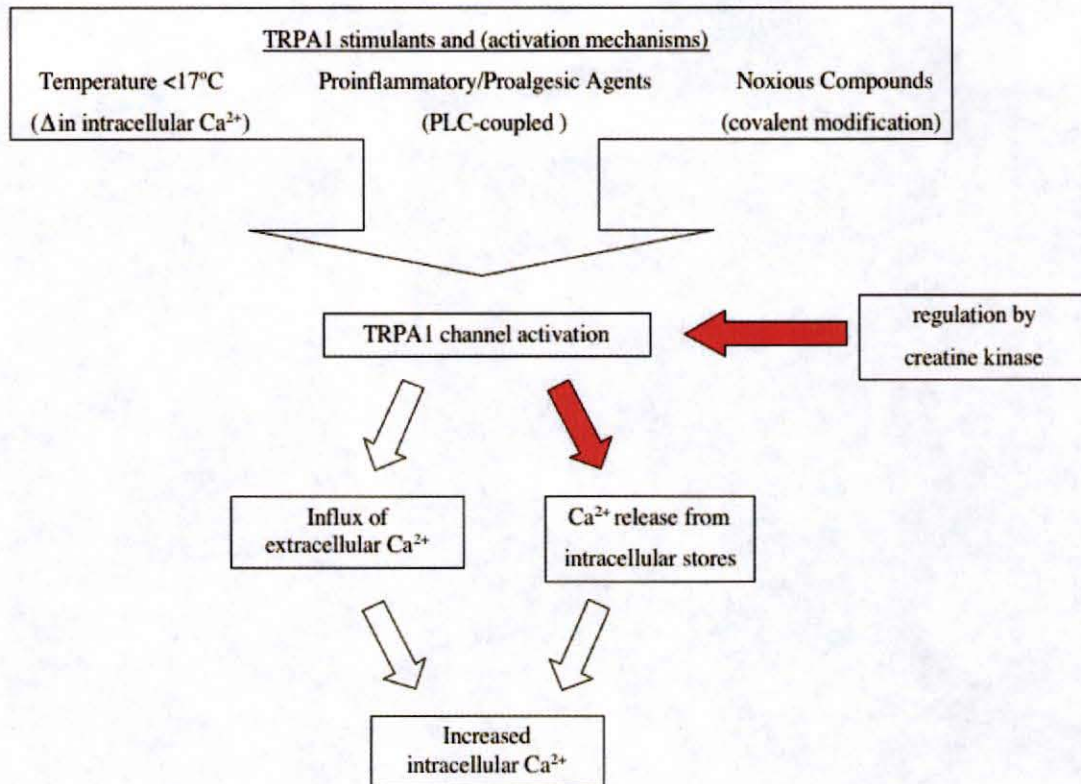


Figure 6.1. Summary graphic.

TRPA1 channel activation by a variety of stimuli is well characterized in the plasma membrane of neuronal cells. The function of TRPA1 channels in the regulation of intracellular calcium levels is also well characterized. Indicated by red arrows, the results presented in this thesis suggest that creatine kinase may regulate TRPA1 channel activity, and that TRPA1 channels may be expressed and function in intracellular membranes.

The results in Chapter 3 show that over-expressed epitope-tagged TRPA1 and creatine kinase interact in HEK cell lysate, which suggests that TRPA1 and creatine kinase may interact *in vivo*. Through its interactions with other ion channels, creatine kinase is involved in the regulation of vital cellular processes. For example, the regulation of cardiac K^+ ATP-sensitive channels by creatine kinase effectively couples the

membrane excitability of guinea pig cardiomyocytes to their metabolic condition. Under conditions of metabolic stress, levels of ADP and phosphocreatine are high in the cell, triggering CK-dependent channel opening with consequent K⁺ efflux, action potential shortening and limitation of intracellular Ca²⁺. (Abraham et al., 2002; Alekseev et al., 2005; Crawford et al., 2002) The regulation of TRPA1 channel activity by creatine kinase *in vivo* could play an equally fundamental role in the regulation of vital cellular processes that are directly linked to energy homeostasis.

Creatine kinase also controls the rate of Ca²⁺ release from mitochondrial stores through a direct interaction with the outer mitochondrial membrane pore (VDAC/Porin). Binding of octameric mitochondrial CK to VDAC inhibits the formation of the permeability transition pore complex and the release of mitochondrial pro-apoptotic factors (Bax dependent release of cytochrome c). In the absence of inhibition by creatine kinase these two events induce apoptosis. The interaction of creatine kinase with VDAC is therefore integral in the control of cell survival. (Brdiczka et al., 1994; Vyssokikh and Brdiczka, 2004; Vyssokikh and Brdiczka, 2003) Creatine kinase might also function as an inhibitor of TRPA1 channel activity, which might prevent increases in intracellular Ca²⁺ levels sufficient to induce apoptosis signaling cascades.

Mitochondrial creatine kinase also functions as an antioxidant by reducing the generation of reactive oxygen species (ROS) through an ADP-recycling mechanism. (Meyer et al., 2006) TRP channels are sensitive to ROS and contribute to hydrogen peroxide (H₂O₂) induced cell death. (Waring, 2005) The over-expression of TRPM and TRPC channels in HEK cells increases the H₂O₂-induced Ca²⁺ influx and corresponding

susceptibilities to oxidative damage and cell death. (Miller, 2006) If the over-expression of TRPA1 has similar consequences, they may be related to the potential interaction with creatine kinase.

The potential regulation of TRPA1 by creatine kinase could be of vital significance to human cells. Therefore, it is important to address whether endogenous TRPA1 and creatine kinase proteins interact *in vivo* and to determine the effect of this interaction on TRPA1 channel activity. The tools described in Chapter 5 will facilitate characterization of the interaction between TRPA1 and creatine kinase proteins.

The results in Chapter 4 show that TRPA1 protein is enriched in human tissues containing smooth muscle where it could possibly be involved in the regulation of contractile movement. This is supported by evidence that TRPA1 activation participates in the graded contractile movement of the rat urinary bladder. (Andrade et al., 2006) In addition, other TRP channels (TRPC1-7, TRPV 2 and 4, TRPP2 and TRPM4 and 7) are expressed in smooth muscle cells where they are involved in the regulation of intracellular calcium levels. Evidence suggests that TRPC channels are involved in the control of blood pressure regulation and may play a role in vascular changes associated with pulmonary hypertension. TRPC1-6, TRPV2 and TRPV4 channels are expressed in airway smooth muscle and may be associated with asthma and chronic obstructive pulmonary disease. (Dietrich et al., 2006) Involvement in pathological conditions and potential means of treatment may be revealed by further characterization of the distribution and role of TRPA1 in human tissues.

TRPA1 protein was also detected in intracellular protein fractions containing mitochondria and ER from human cells; however, the results from preliminary cell-based calcium assays designed to explore the function of TRPA1 in intracellular membranes were inconclusive (see Chapter 4 and Appendix A). Mitochondria and the ER can serve as intracellular Ca^{2+} stores and several members of the TRP channel family of proteins are involved in the release of Ca^{2+} from intracellular stores. Variant splicing of TRPM8 results in a truncated protein that is retained in the ER where it functions as a Ca^{2+} release channel. (Bidaux et al., 2007) TRPV1 is expressed in and functions in Ca^{2+} release from intracellular stores. (Hagenacker et al., 2007; Turner et al., 2003) Recent research also suggests a role for TRPV2 in early endosomes. (Saito et al., 2007) It is possible that TRPA1 could play a similar role in the release of Ca^{2+} from intracellular stores, thus it could contribute to the regulation of vital cell functions and possibly initiate cell death pathways.

The involvement of TRPA1 activation in the calcium-induced initiation of cell death pathways could also be inferred by the diverse array of noxious environmental stimuli that activate the channel. This is the case for TRPV1 channels, which contribute to microglial cell death via Ca^{2+} signaling and mitochondrial disruption. (Kim et al., 2006) One TRPA1 stimulating compound, cinnamaldehyde, has been shown to induce apoptosis in a number of human cancer cells. (Wu et al., 2004) Benzyl isothiocyanate (BITC) is another TRPA1-activating chemical that causes cytotoxic increases in the Ca^{2+} membrane permeability of mammalian vascular smooth muscle. (Wilson et al., 2002) Painfully cold temperatures also stimulate TRPA1 to induce an increase in mitochondrial

calcium levels, resulting in ischemic tissue damage and apoptosis. (Anderson et al., 2004)

The activation of TRPA1 by these various stimuli could be responsible for increases in intracellular calcium that lead to cell death.

The potential involvement of TRPA1 in the initiation of cell death pathways could be examined by growth curve and apoptosis assays. The involvement of TRPA1 in the regulation of release from mitochondria could be examined using JC-1 dye to determine whether TRPA1 activation has an effect on mitochondrial depolarization.

All of these functions proposed for TRPA1 provide compelling reasons to continue investigating potential novel roles of TRPA1 channel.

APPENDIX A

Functional Assays

Identification of TRPA1 in multiple subcellular fractions suggests that it may play a role in the regulation of calcium levels in intracellular stores. Spectrophotometric Fura-2 assays were designed to test this hypothesis *in Vivo*.

Specific Methods

Fura-2 calcium assay

HEK and AFC cells were loaded with 4mM Fura-2 AM (Molecular Probes) in a 1:1 mix of conditioned media and calcium free ringer buffer for 45 min at 37°C. Cells were washed with calcium free ringer buffer and harvested by trypsinization, spun 5 minutes at 200 x g and re-suspended in calcium free ringer (2×10^6 cells/ml). Calcium flux was measured in 3ml volumes of cells suspended in ringer solution. Changes in Fura-2 fluorescence were measured at 510 nM on a Perkin Elmer luminescence spectrometer (LS 50 B) and analyzed with the associated FLWIN software (version 2.0). Assays were performed in the absence and presence of external calcium (not shown). Thapsigargin (1mM) and ionomycin (500 nM) were used as positive controls respectively for the release of calcium from intracellular stores and for permeabilization of the plasma membrane.

Results and Discussion

Thapsigargin and ionomycin elicited the predicted responses corresponding to the release of calcium from intracellular stores and for permeabilization of the plasma membrane in both HEK and AFC cells. When extra-cellular calcium was present, Benzyl-isothiocyanate (BITC, Figure A) elicited an increase in intracellular calcium that may correspond to the activation of TRPA1 in the plasma membrane of AFC cells. This response was not observed in HEK cells nor was it observed in the absence of extra-cellular calcium. These results were not consistently replicated. Failure of BITC to elicit a response in the absence of external calcium may indicate the following: that this compound specifically activates TRPA1 only at the plasma membrane, that the compound was unable to access intracellular locations where it could activate TRPA1 or that TRPA1 is located only at the plasma membrane. Further research must be done to determine the role of TRPA1 in the regulation of calcium levels in intracellular compartments.

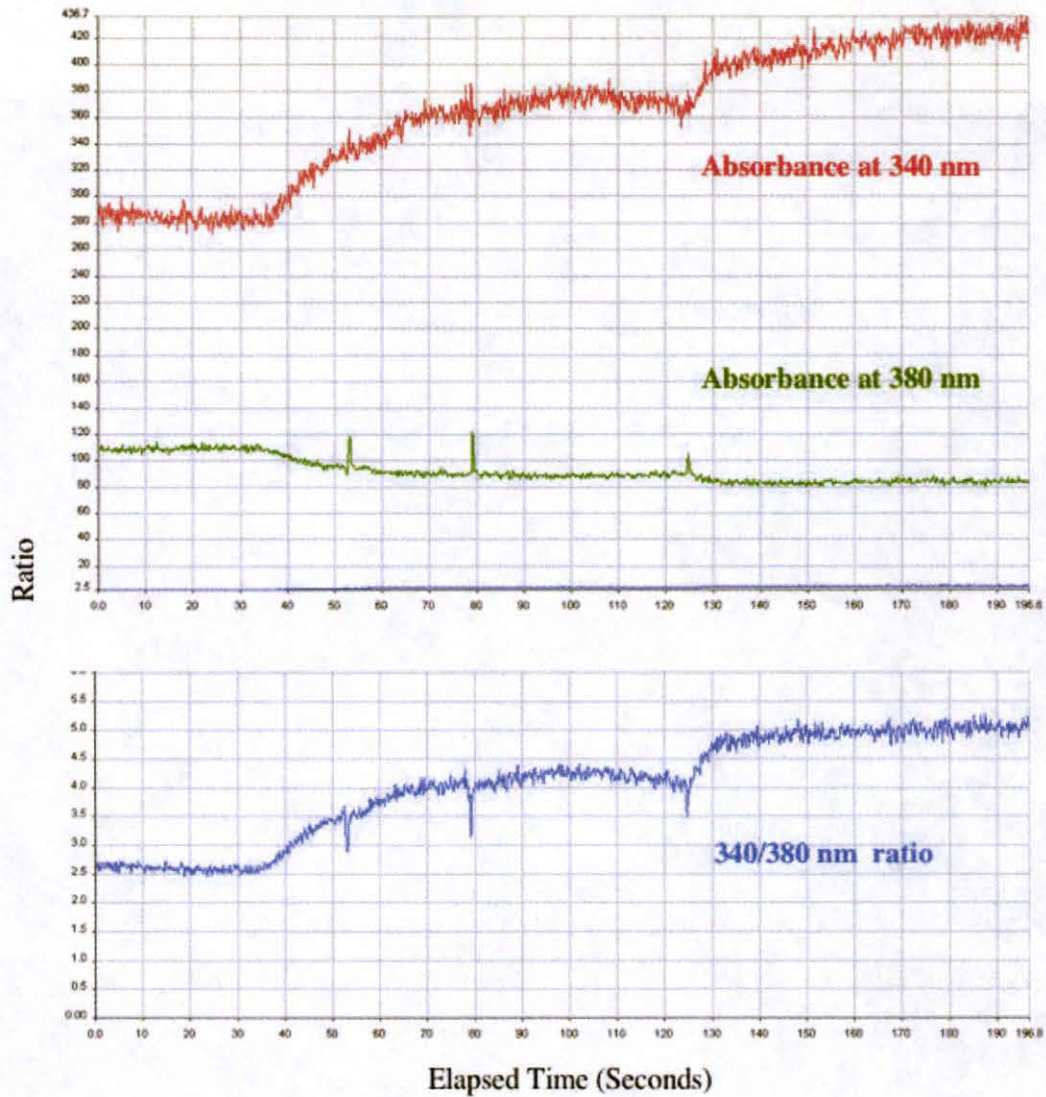


Figure A.1 Changes in FURA-2 AM absorbance in BITC-stimulated AFC cells.

In this representative plot, BITC (200 μ M) was added at 25, 50 and 150 sec, and thapsigargin (0.5 μ M) at 175 seconds to AFC cells loaded with Fura-2 AM dye. This experiment was performed in ringier solution with external calcium. Red line represents the absorbance at 340nm, green line represents the absorbance at 380 nm, and blue line (blown up in bottom plot) represents the ratio of absorbance at 340/380 nm. Changes in absorbance values indicate changes in intracellular calcium levels resulting from the activation of TRPA1 channels on the surface of AFC cells in response to the addition of benzyl isothiocyanate (BITC).

APPENDIX B

Affinity Binding Assays

The his-tagged proteins described in Chapter 5 have been used in affinity binding assays to explore the nature of the interaction between TRPA1 and CKM. The assays were designed to determine whether the C and N terminals of TRPA1 are able to interact directly with one another and with CKM in an *in vitro* environment. This would support a direct interaction between TRPA1 and CKM *in Vivo* as opposed to an indirect association as components of an intracellular complex.

Specific Methods

Affinity Matrix Binding. Dialyzed His-Tagged proteins were coupled to Affigel-10 affinity matrix (BioRad, CA) for 4 hr at 4°C. The potentially active ester binding sites on the Affigel were blocked by addition 1M ethanolamine HCl pH 8 (0.1 ml/ml gel) for 1 hr at 4°C. Next, the gel was washed with 10 volumes deionized H₂O, then with five volumes 5 M NaCl and resuspended in 1X Lysis Buffer (10mM Tris-HCl pH 7.4, 1mM phenylmethylsulfonyl fluoride, 10mM iodoacetamide, and 25mM NaCl).

***In vitro* affinity assay.** Eppendorf tubes were prepared containing 200 µl (~10 µg) of the coupled His-tagged proteins. Candidate interacting His-tagged proteins (100 µl) were added to the tubes which were rotated 4hr at 4 °C. After affinity purification, the protein complexes were harvested by centrifugation (15,000 x g for 1 min at RT), followed by three washes in 1 ml of ice-cold Lysis Buffer. After the final wash, the beads were dried

using a Hamilton syringe, re-suspended in 100 μ l of reducing Laemmli sample buffer, and heated at 95 °C for 8 min. Complexes were examined by SDS-PAGE and Western Blot.

Results and Discussion

Post-purification samples were too dilute after dialysis to allow for accurate protein quantification by the D_c assay. The quantification protein in the post-coupling affinity complexes was hindered by the presence of residual compound contamination and the basic pH (10) of these samples. Approximate protein concentrations were determined by ultraviolet absorbance and the following equation:

$$[\text{Protein}] \text{ (mg/mL)} = 1.55 * A_{280} - 0.76 * A_{260}$$

Two major difficulties were encountered that prevented determination of the nature of the interaction *in vitro*. First, positive binding signals were detected in negative controls where blocked affinity beads seem to be binding to proteins. Second, background results from the release of protein covalently bound to affinity beads. The representative western blot shown in Figure B.1 demonstrates the difficulties experienced in *in vitro* assays.

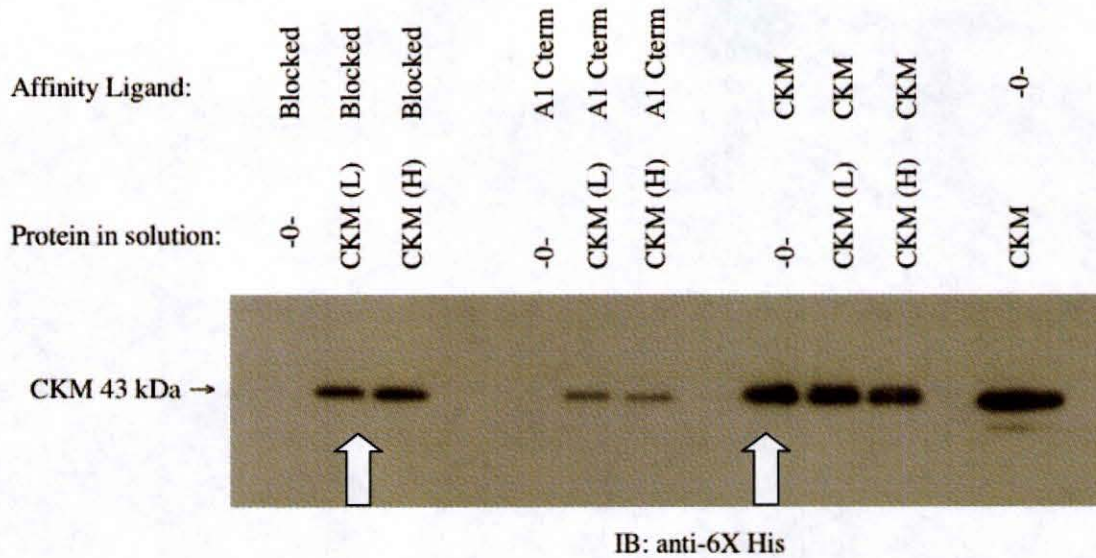


Figure B.1. Preliminary *in vitro* affinity binding assay.

Dialyzed His-Tagged CKM and TRPA1 C-terminal proteins were coupled to an affinity matrix. Additional potentially active ester binding sites were blocked by addition of 1M ethanolamine HCl pH 8 (0.1 ml/ml gel). The coupled His-tagged proteins (200 μ l) were incubated with uncoupled His-tagged proteins (100 μ l) for 4hr at 4 °C. Protein complexes were harvested by centrifugation, re-suspended in RSB, separated by SDS-10% PAGE and detected western blot with anti-6X-histidine. Left arrow indicates that His-tagged CKM protein was detected in negative controls where the affinity ligand is blocked affinity matrix. Right arrow indicates that His-tagged CKM protein was also observed in the sample where unbound CKM protein in solution is not present.

Difficulties might be reduced in future experiments by using a different substrate, such as, Protein A agarose or by recoupling the His-proteins to resin from the His-Bind purification kit (Novagen).

REFERENCES

- Abraham, M. R., Selivanov, V. A., Hodgson, D. M., Pucar, D., Zingman, L. V., Wieringa, B., Dzeja, P. P., Alekseev, A. E., and Terzic, A. (2002). Coupling of cell energetics with membrane metabolic sensing. Integrative signaling through creatine kinase phosphotransfer disrupted by M-CK gene knock-out. *J Biol Chem* *277*, 24427-24434.
- Alekseev, A. E., Hodgson, D. M., Karger, A. B., Park, S., Zingman, L. V., and Terzic, A. (2005). ATP-sensitive K⁺ channel channel/enzyme multimer: metabolic gating in the heart. *J Mol Cell Cardiol* *38*, 895-905.
- Anderson, C. D., Belous, A., Pierce, J., Nicoud, I. B., Knox, C., Wakata, A., Pinson, C. W., and Chari, R. S. (2004). Mitochondrial calcium uptake regulates cold preservation-induced Bax translocation and early reperfusion apoptosis. *Am J Transplant* *4*, 352-362.
- Andrade, E. L., Ferreira, J., Andre, E., and Calixto, J. B. (2006). Contractile mechanisms coupled to TRPA1 receptor activation in rat urinary bladder. *Biochem Pharmacol* *72*, 104-114.
- Bandell, M., Story, G. M., Hwang, S. W., Viswanath, V., Eid, S. R., Petrus, M. J., Earley, T. J., and Patapoutian, A. (2004). Noxious cold ion channel TRPA1 is activated by pungent compounds and bradykinin. *Neuron* *41*, 849-857.
- Bautista, D. M., Jordt, S. E., Nikai, T., Tsuruda, P. R., Read, A. J., Poblete, J., Yamoah, E. N., Basbaum, A. I., and Julius, D. (2006). TRPA1 mediates the inflammatory actions of environmental irritants and proalgesic agents. *Cell* *124*, 1269-1282.
- Bidaux, G., Flourakis, M., Thebault, S., Zholos, A., Beck, B., Gkika, D., Roudbaraki, M., Bonnal, J. L., Mauroy, B., Shuba, Y., *et al.* (2007). Prostate cell differentiation status determines transient receptor potential melastatin member 8 channel subcellular localization and function. *J Clin Invest* *117*, 1647-1657.
- Brdiczka, D., Kaldis, P., and Wallimann, T. (1994). In vitro complex formation between the octamer of mitochondrial creatine kinase and porin. *J Biol Chem* *269*, 27640-27644.
- Clapham, D. E. (2003). TRP channels as cellular sensors. *Nature* *426*, 517-524.
- Clapham, D. E., Runnels, L. W., and Strubing, C. (2001). The TRP ion channel family. *Nat Rev Neurosci* *2*, 387-396.
- Corey, D. P., Garcia-Anoveros, J., Holt, J. R., Kwan, K. Y., Lin, S. Y., Vollrath, M. A., Amalfitano, A., Cheung, E. L., Derfler, B. H., Duggan, A., *et al.* (2004). TRPA1 is a

candidate for the mechanosensitive transduction channel of vertebrate hair cells. *Nature* **432**, 723-730.

Crawford, R. M., Ranki, H. J., Botting, C. H., Budas, G. R., and Jovanovic, A. (2002). Creatine kinase is physically associated with the cardiac ATP-sensitive K⁺ channel in vivo. *FASEB J* **16**, 102-104.

Dietrich, A., Chubanov, V., Kalwa, H., Rost, B. R., and Gudermann, T. (2006). Cation channels of the transient receptor potential superfamily: their role in physiological and pathophysiological processes of smooth muscle cells. *Pharmacol Ther* **112**, 744-760.

Doerner, J. F., Gisselmann, G., Hatt, H., and Wetzell, C. H. (2007). Transient receptor potential channel A1 is directly gated by calcium ions. *J Biol Chem* **282**, 13180-13189.

Hagenacker, T., Ledwig, D., and Busselberg, D. (2007). Feedback mechanisms in the regulation of intracellular calcium ([Ca²⁺]_i) in the peripheral nociceptive system: Role of TRPV-1 and pain related receptors. *Cell Calcium*.

Hill, K., and Schaefer, M. (2007). TRPA1 is differentially modulated by the amphipathic molecules trinitrophenol and chlorpromazine. *J Biol Chem* **282**, 7145-7153.

Hinman, A., Chuang, H. H., Bautista, D. M., and Julius, D. (2006). TRP channel activation by reversible covalent modification. *Proc Natl Acad Sci U S A* **103**, 19564-19568.

Jacobson, J., and Duchon, M. R. (2004). Interplay between mitochondria and cellular calcium signalling. *Mol Cell Biochem* **256-257**, 209-218.

Jaquemar, D., Schenker, T., and Trueb, B. (1999). An ankyrin-like protein with transmembrane domains is specifically lost after oncogenic transformation of human fibroblasts. *J Biol Chem* **274**, 7325-7333.

Jordt, S. E., Bautista, D. M., Chuang, H. H., McKemy, D. D., Zygmunt, P. M., Hogestatt, E. D., Meng, I. D., and Julius, D. (2004). Mustard oils and cannabinoids excite sensory nerve fibres through the TRP channel ANKTM1. *Nature* **427**, 260-265.

Julius, D., and Basbaum, A. I. (2001). Molecular mechanisms of nociception. *Nature* **413**, 203-210.

Kim, D., and Cavanaugh, E. J. (2007). Requirement of a soluble intracellular factor for activation of transient receptor potential A1 by pungent chemicals: role of inorganic polyphosphates. *J Neurosci* **27**, 6500-6509.

- Kim, S. R., Kim, S. U., Oh, U., and Jin, B. K. (2006). Transient receptor potential vanilloid subtype 1 mediates microglial cell death in vivo and in vitro via Ca²⁺-mediated mitochondrial damage and cytochrome c release. *J Immunol* *177*, 4322-4329.
- Kwan, K. Y., Allchorne, A. J., Vollrath, M. A., Christensen, A. P., Zhang, D. S., Woolf, C. J., and Corey, D. P. (2006). TRPA1 contributes to cold, mechanical, and chemical nociception but is not essential for hair-cell transduction. *Neuron* *50*, 277-289.
- Kyte, J., and Doolittle, R. F. (1982). A simple method for displaying the hydropathic character of a protein. *J Mol Biol* *157*, 105-132.
- Macpherson, L. J., Dubin, A. E., Evans, M. J., Marr, F., Schultz, P. G., Cravatt, B. F., and Patapoutian, A. (2007). Noxious compounds activate TRPA1 ion channels through covalent modification of cysteines. *Nature* *445*, 541-545.
- Mahieu, F., Owsianik, G., Verbert, L., Janssens, A., De Smedt, H., Nilius, B., and Voets, T. (2007). TRPM8-independent menthol-induced Ca²⁺ release from endoplasmic reticulum and Golgi. *J Biol Chem* *282*, 3325-3336.
- Meyer, L. E., Machado, L. B., Santiago, A. P., da-Silva, W. S., De Felice, F. G., Holub, O., Oliveira, M. F., and Galina, A. (2006). Mitochondrial creatine kinase activity prevents reactive oxygen species generation: antioxidant role of mitochondrial kinase-dependent ADP re-cycling activity. *J Biol Chem* *281*, 37361-37371.
- Miller, B. A. (2006). The role of TRP channels in oxidative stress-induced cell death. *J Membr Biol* *209*, 31-41.
- Minke, B., and Cook, B. (2002). TRP channel proteins and signal transduction. *Physiol Rev* *82*, 429-472.
- Montell, C. (2001). Physiology, phylogeny, and functions of the TRP superfamily of cation channels. *Sci STKE* *2001*, RE1.
- Moran, M. M., Xu, H., and Clapham, D. E. (2004). TRP ion channels in the nervous system. *Curr Opin Neurobiol* *14*, 362-369.
- Nicholls, D. G. (2005). Mitochondria and calcium signaling. *Cell Calcium* *38*, 311-317.
- Nilius, B. (2007). TRP channels in disease. *Biochim Biophys Acta* *1772*, 805-812.
- Parekh, A. B. (2003). Mitochondrial regulation of intracellular Ca²⁺ signaling: more than just simple Ca²⁺ buffers. *News Physiol Sci* *18*, 252-256.
- Pedersen, S. F., Owsianik, G., and Nilius, B. (2005). TRP channels: an overview. *Cell Calcium* *38*, 233-252.

- Peretz, A., Sandler, C., Kirschfeld, K., Hardie, R. C., and Minke, B. (1994). Genetic dissection of light-induced Ca²⁺ influx into Drosophila photoreceptors. *J Gen Physiol* 104, 1057-1077.
- Peterlin, Z., Chesler, A., and Firestein, S. (2007). A painful trp can be a bonding experience. *Neuron* 53, 635-638.
- Ramsey, I. S., Delling, M., and Clapham, D. E. (2006). An introduction to TRP channels. *Annu Rev Physiol* 68, 619-647.
- Saito, M., Hanson, P. I., and Schlesinger, P. (2007). Luminal chloride-dependent activation of endosome calcium channels: patch clamp study of enlarged endosomes. *J Biol Chem* 282, 27327-27333.
- Saito, S., and Shingai, R. (2006). Evolution of thermoTRP ion channel homologs in vertebrates. *Physiol Genomics* 27, 219-230.
- Schnyder, T., Rojo, M., Furter, R., and Wallimann, T. (1994). The structure of mitochondrial creatine kinase and its membrane binding properties. *Mol Cell Biochem* 133-134, 115-123.
- Stokes, A., Wakano, C., Koblan-Huberson, M., Adra, C. N., Fleig, A., and Turner, H. (2006). TRPA1 is a substrate for de-ubiquitination by the tumor suppressor CYLD. *Cell Signal* 18, 1584-1594.
- Story, G. M., Peier, A. M., Reeve, A. J., Eid, S. R., Mosbacher, J., Hricik, T. R., Earley, T. J., Hergarden, A. C., Andersson, D. A., Hwang, S. W., *et al.* (2003). ANKTM1, a TRP-like channel expressed in nociceptive neurons, is activated by cold temperatures. *Cell* 112, 819-829.
- Turner, H., Fleig, A., Stokes, A., Kinet, J. P., and Penner, R. (2003). Discrimination of intracellular calcium store subcompartments using TRPV1 (transient receptor potential channel, vanilloid subfamily member 1) release channel activity. *Biochem J* 371, 341-350.
- Van Crielinge, W., and Beyaert, R. (1999). Yeast Two-Hybrid: State of the Art. *Biol Proced Online* 2, 1-38.
- Venkatachalam, K., and Montell, C. (2007). TRP channels. *Annu Rev Biochem* 76, 387-417.
- Vyssokikh, M., and Brdiczka, D. (2004). VDAC and peripheral channelling complexes in health and disease. *Mol Cell Biochem* 256-257, 117-126.

- Vyssokikh, M. Y., and Brdiczka, D. (2003). The function of complexes between the outer mitochondrial membrane pore (VDAC) and the adenine nucleotide translocase in regulation of energy metabolism and apoptosis. *Acta Biochim Pol* 50, 389-404.
- Waring, P. (2005). Redox active calcium ion channels and cell death. *Arch Biochem Biophys* 434, 33-42.
- Webb, T., Jackson, P. J., and Morris, G. E. (1997). Protease digestion studies of an equilibrium intermediate in the unfolding of creatine kinase. *Biochem J* 321 (Pt 1), 83-88.
- Wilson, R. K., Kwan, T. K., Kwan, C. Y., and Sorger, G. J. (2002). Effects of papaya seed extract and benzyl isothiocyanate on vascular contraction. *Life Sci* 71, 497-507.
- Wu, S. J., Ng, L. T., and Lin, C. C. (2004). Effects of vitamin E on the cinnamaldehyde-induced apoptotic mechanism in human PLC/PRF/5 cells. *Clin Exp Pharmacol Physiol* 31, 770-776.
- Zurborg, S., Yurgionas, B., Jira, J. A., Caspani, O., and Heppenstall, P. A. (2007). Direct activation of the ion channel TRPA1 by Ca²⁺. *Nat Neurosci* 10, 277-279.